



# Delineating the main structural outlines and the petrophysical properties of the Albian-upper Cretaceous Reservoirs using seismic and well log data, Shushan Basin, north Western Desert, Egypt

Nancy H. El Dally<sup>1</sup> · Mahmoud S. Youssef<sup>1</sup> · Mohamed H. Abdel Aal<sup>2</sup> · Farouk I. Metwalli<sup>3</sup> · Bassem S. Nabawy<sup>4</sup>

Received: 23 May 2022 / Accepted: 30 December 2022 / Published online: 7 January 2023  
© The Author(s) 2023

## Abstract

This study concerns with delineating and analyzing the subsurface structural setting of Khalda Oil Field at Shushan Basin as a key factor for evaluating the petrophysical properties and the deliverability of the Bahariya Formation. Shushan Basin is considered one of the most prospective basins in the Western Desert. The oil is trapped within a gentle seismically defined anticline that contains a series of coastal sandstone reservoirs interbedded with a neritic and tidal flat mudstone and a few carbonate interbeds of the Albian-Cenomanian Bahariya Formation forming multiple oil-bearing sandstone reservoirs. A set of borehole logging and seismic data were available, tied, processed, and mapped to delineate the predominant structures in the study area. Results show the implication of the NW–SE, NE–SW, and E–W gravity faulting on the Bahariya and the overlying Abu Roash formations. This set of gravity faults is attributed to the Mesozoic tensional stresses. The depth structure contour maps on the upper surfaces of the Lower and Upper Bahariya members reveal the presence of some NE–SW gravity faults that dissected the Khalda Field into some slightly tilted blocks, shallowing in depth to the south as deepening to the north. Besides, the study area has been affected later in the Jurassic by E–W gravity faults during the Atlantic Ocean opening. This faulting trend was changed later into the NE–SW direction as a result of the movement of North Africa against Laurasia. The petrophysical analysis indicated that the Lower Bahariya sandstone reservoir has a good reservoir quality ( $16 \leq \varnothing \leq 25\%$ ,  $53 \leq S_w \leq 59\%$ ,  $6.0 \leq V_{sh} \leq 32.2\%$ , and good net-pay thickness 18.0–38.0 ft). It is revealed that the drilled wells penetrating the crest of the anticline are prospective while that located in the anticline flanks are water-bearing recommending exploration away from the anticline flanks. By applying this workflow, it is possible to explore for the similar subsurface hydrocarbons-bearing sequences in the Western Desert and North Africa in future exploitation plans.

**Keywords** Bahariya Formation · Shushan Basin · Structural setting · Seismic interpretation · Petrophysical properties · Clastic sequence

## List of symbols

$a$	Lithology factor, 0.0
$m$	Porosity exponent, 0.0
$\Delta T_f$	Sonic fluid velocity, $\mu\text{s}/\text{ft}$
$\Delta T_{\log}$	Sonic velocity from log, $\mu\text{s}/\text{ft}$

$\varnothing$	Porosity, %
$\varnothing_{\text{DLog}}$	Density porosity log reading, 0.0
$\varnothing_e$	Effective porosity, %
$\varnothing_{\text{Nf}}$	Neutron porosity of the saturating fluid, 0.0
$\varnothing_{\text{NLog}}$	Neutron porosity log reading, 0.0
$\varnothing_T$	Total porosity, 0.0;
$\rho_f$	Fluid density, $\text{g}/\text{cc}$
$\rho_{\text{Log}}$	Density log reading; $\text{g}/\text{cc}$

✉ Bassem S. Nabawy  
bsnabawy@yahoo.co.uk

- <sup>1</sup> Geology Department, Faculty of Science, Ain Shams University, Cairo, Egypt
- <sup>2</sup> Geology Department, Faculty of Education, Ain Shams University, Cairo, Egypt
- <sup>3</sup> Geology Department, Faculty of Science, Helwan University, Cairo, Egypt
- <sup>4</sup> Geophysical Sciences Department, National Research Center, Cairo, Egypt

## List of Acronyms

$\text{GR}_{\text{LOG}}$	Gamma-ray log reading, API
$\text{GR}_{\text{MAX}}$	The maximum gamma-ray reading, API
$\text{GR}_{\text{MIN}}$	The minimum gamma-ray reading, API
Rsh	Shale resistivity, ohm
RT	True resistivity, ohm
Rw	Water resistivity, ohm
SQRT	Square root of a given value

Sw Water Saturation, 0.0  
 Vsh Southwest Mesopotamian

## Introduction

The Sedimentary basins of the Western Desert (WD) in Egypt are among the most prolific areas for hydrocarbon exploitation in North Africa. The WD is bounded to the north by the Mediterranean shorelines and extends for 600 km from the Libyan borders in the west to the Nile Valley in the east. The sedimentary basins in the north WD are aged as Mesozoic and Early Tertiary basins, which have been variously described as the Northern Basins or the Coastal Basins. They lie to the north of Qattara Ridge which is known as Sharib-Sheila High which separates these northern basins from the Abu Gharadig Basin in the center of the WD (Fig. 1). These Coastal Basins comprise four discrete Mesozoic basins: Matruh and Shushan Basins to the west, while to east the Dahab/Mireir and Natrun basins are situated (Fig. 1). The hydrocarbons have been trapped in these basins within structural traps that follow the Syrian Arc structural trend. These traps are formed as fault-blocks, and three to four way closure structures (Teama and Nabawy 2016; Shehata et al. 2020, 2021; Nabawy et al. 2022).

The Shushan Basin contains a northward thickening Mesozoic and Tertiary section, which unconformably

overlies the thick Paleozoic sediments of Siwa Basin to the west near the Libyan borders (EGPC 1992). It contains two prominent Jurassic to Lower Cretaceous grabens, namely, the NE-SW Shushan Trough, and the triangular-shaped Matruh Trough, which is defined by a combination of NE–SW and NNE–SSW faults.

The Cretaceous Bahariya Formation with its dominant clastic composition and regional extension is considered among the most prolific formations in the coastal Basins of the north Western Desert, and in particular the Shushan Basin. Also, it is considered among the highly heterogeneous lithologies in Egypt; it is composed of intermixed medium to coarse-grained sandstones and shales with a few carbonate interbeds (Abu Shady et al. 2010). Therefore, it has been intensively studied in the different coastal basins, but it is still in need to more detailed studies in Shushan Basin and particularly in in Khalda Oil Field (Hassan et al. 2015; Nabawy et al. 2022). However, reservoir characterization based on integrated seismic and petrophysical data was widely by many authors in different areas in all over the world (Emujakporue et al. 2012; Maity and Aminzadeh 2012, 2015; Mohamed et al. 2016; Wang et al. 2017; Abdelmaksoud, and Radwan 2022). Thereby, a detailed structural study, based on two-way-time seismic data, is of critical importance to support the future development and exploration plans in the Northern Basins in NW Africa.



**Fig. 1** Location map of the Khalda Oil Field and the Coastal Basins in north Western Desert, Egypt (Rossi et al. 2001)

### Lithostratigraphy

The Lower Cretaceous lithostratigraphic formations in the studied sequence are represented by Abu Roash, Bahariya, Kharita, Alamein, and Alam El Bueib formations (Fig. 2). Alam El Bueib Formation consists of siltstone, shale, sandstone, dolostone, and limestone intercalations. The sandstone interbeds are prospective as hydrocarbons-bearing zones, whereas the shale beds are considered source rocks. The Aptian Alamein Formation consists of dolostones with some shale and limestone interbeds that have been deposited in a marine transgression (Schlumberger 1995). Upwards, the Albian Kharita Formation consists primarily of fluvial medium to coarse-grained sandstone and friable sand intercalated with thin siltstone and shale layers. It is overlain by the Albian-Cenomanian Bahariya Formation.

The Bahariya Formation, the core of the present study, in Khalda Oil Field is primarily hydrocarbon-bearing

sandstone sequences. Upwards the Abu Roash Formation is built of interbedded shale and limestone, intercalated with some thin siltstone, sandstone, and anhydrite interbeds. The Bahariya Formation is the most promising oil-bearing reservoirs in Khalda Oil Field. It is primarily composed of sandstone facies accumulated in a transgressive shallow marine coastal depositional setting, with some neritic shales and thin carbonate interbeds. The Bahariya Formation is divided into upper and lower members (Fig. 2) and reaches up to 1013 ft thick in Khalda-1 well (EGPC 1992). Thickness of the Upper Bahariya Member is several hundred feet and is mainly composed of shale and thin beds of limestone, whereas the Lower Bahariya Member is thick and composed of sandstone and shale interbeds. The Upper Bahariya Member in the North Western Desert has been studied sedimentologically in detail by many authors (e.g., Almoqaddam et al. 2018; Kassab et al. 2019; Abdelmaksoud et al. 2019; Nabawy et al. 2022). Besides, the Upper Bahariya Member in Khalda Oil Field

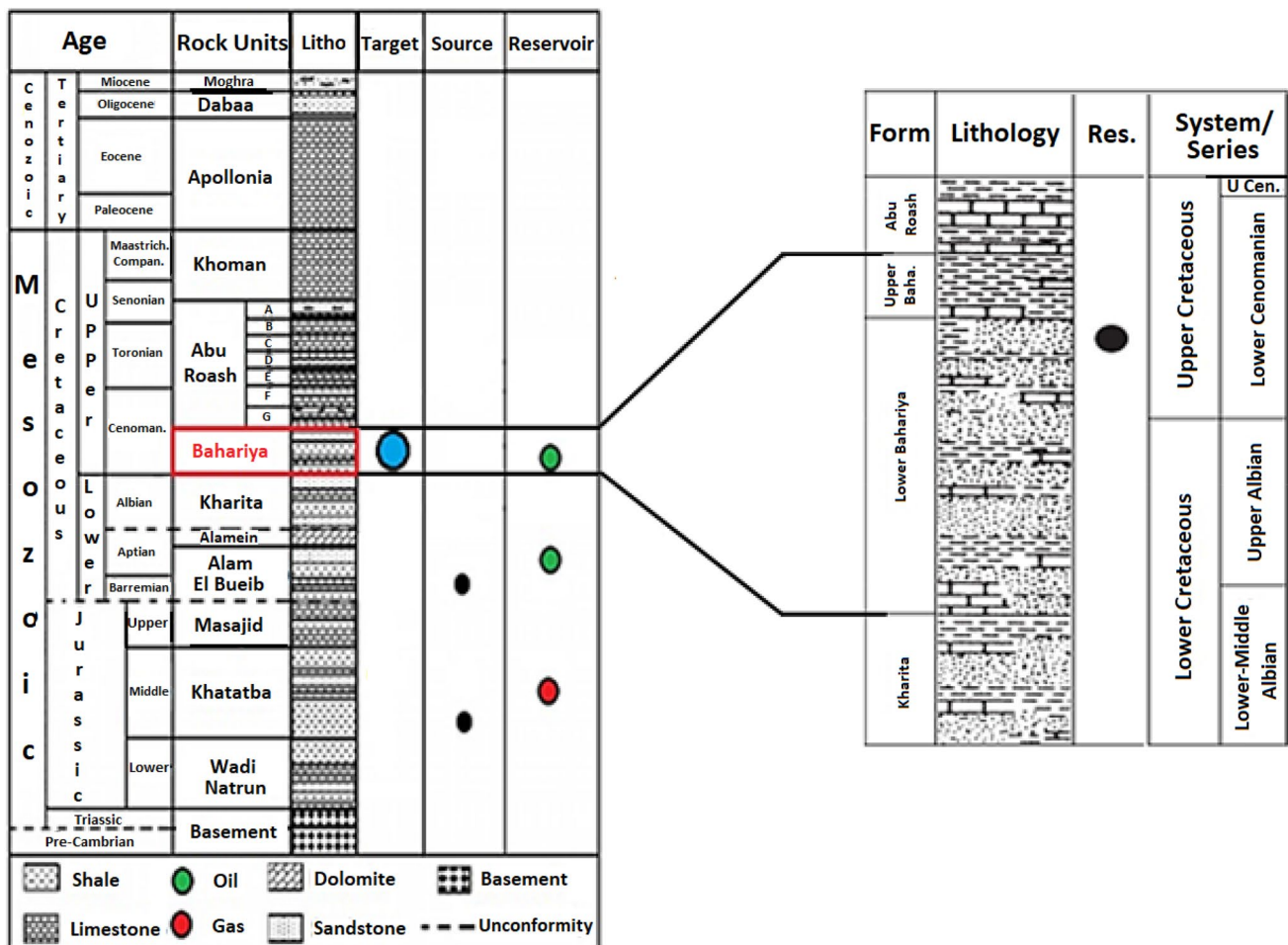


Fig. 2 A generalized stratigraphic column of the Khalda Oil Field in the Western Desert with a detailed sketch for the Bahariya Formation (Schlumberger 1995)

acts as a seal rock that effectively traps the oil in the sandstones of the Lower Bahariya. It overlies unconformably the Middle Jurassic Khatatba Formation which consists of three depositional units: upper shale/siltstone, middle sandstone, and lower shale unit. The lower and upper shale units are considered the prime source rocks for producing the trapped oil in Khalda structure (EGPC 1992).

## Structure setting

The Khalda Oil Field occurs at the northern end of the Shushan Trough which subsided rapidly during the Jurassic and Early Cretaceous. The Shushan Trough is mostly defined by a set of NE–SW faults which is mostly recognized on top of the Upper Jurassic Masajid horizon (Fig. 2), and less commonly on top of the Aptian-Alamein dolomite. These rift-bounding faults were apparently sealed shortly after the deposition of the Alamein Formation, so the structural map on top of the Cenomanian Bahariya reservoir does not reveal the presence of these deep-seated grabens (Fig. 3). The detailed morphology of the Shushan Trough is poorly known because seismic data quality below 2.5 s is poor (Abdou 1998). However, the structural framework

of the Late Cretaceous-Tertiary sequence is dominated by the ESE–WNW or E–W dextral strike-slip faults, and the SE–NW gravity faults that have been formed during the Upper Cretaceous-Eocene Syrian Arc tectonic event (Fig. 3).

The setting of Khalda structure may have been controlled by deep-seated NE–SW normal faults associated with the Shushan Trough (Fig. 4), which were subjected to NW–SE compression during the ‘Syrian Arc’ tectonic phase. This same compressive phase is responsible for the anticlinal nature of the field (Fig. 5).

The Khalda structure on top of the Bahariya reservoir is represented by a gentle slope anticline oriented NE–SW of 5.5 km length and 2 km width. The remarkably rectilinear east flank has a pronounced NNE–SSW trend, and is steeper (up to 60°) than the irregular W to NW flank (dips up to 30°). The structure is cut by some normal SE–NW faults and WNW–ESE dextral strike-slip faults (Sehim et al. 1992) (Fig. 6). The faults have thrown the cut beds for more than 50 ft with some sealing implication which is noticeably situated at the southern borders of the Khalda structure (EGPC 1992). The highest point on the structure occurs in the south of the anticline, in the vicinity of Khalda-2 and -4 wells, and is apparently associated with a significant NW–SE cross-fault.

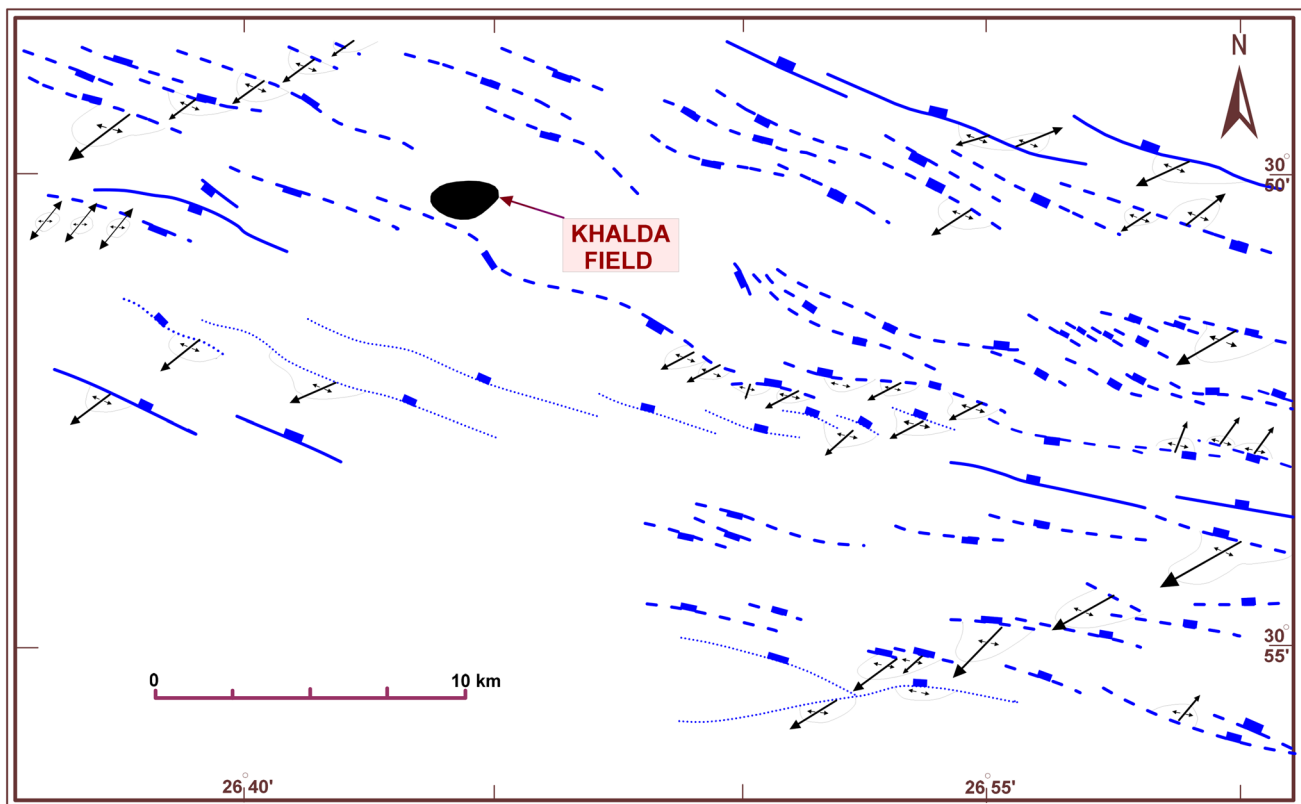


**Fig. 3** Structural sketch map for the Khalda Concession showing the main faults and structural closures at the top of the Cenomanian Bahariya sequence (Sehim et al. 1992)

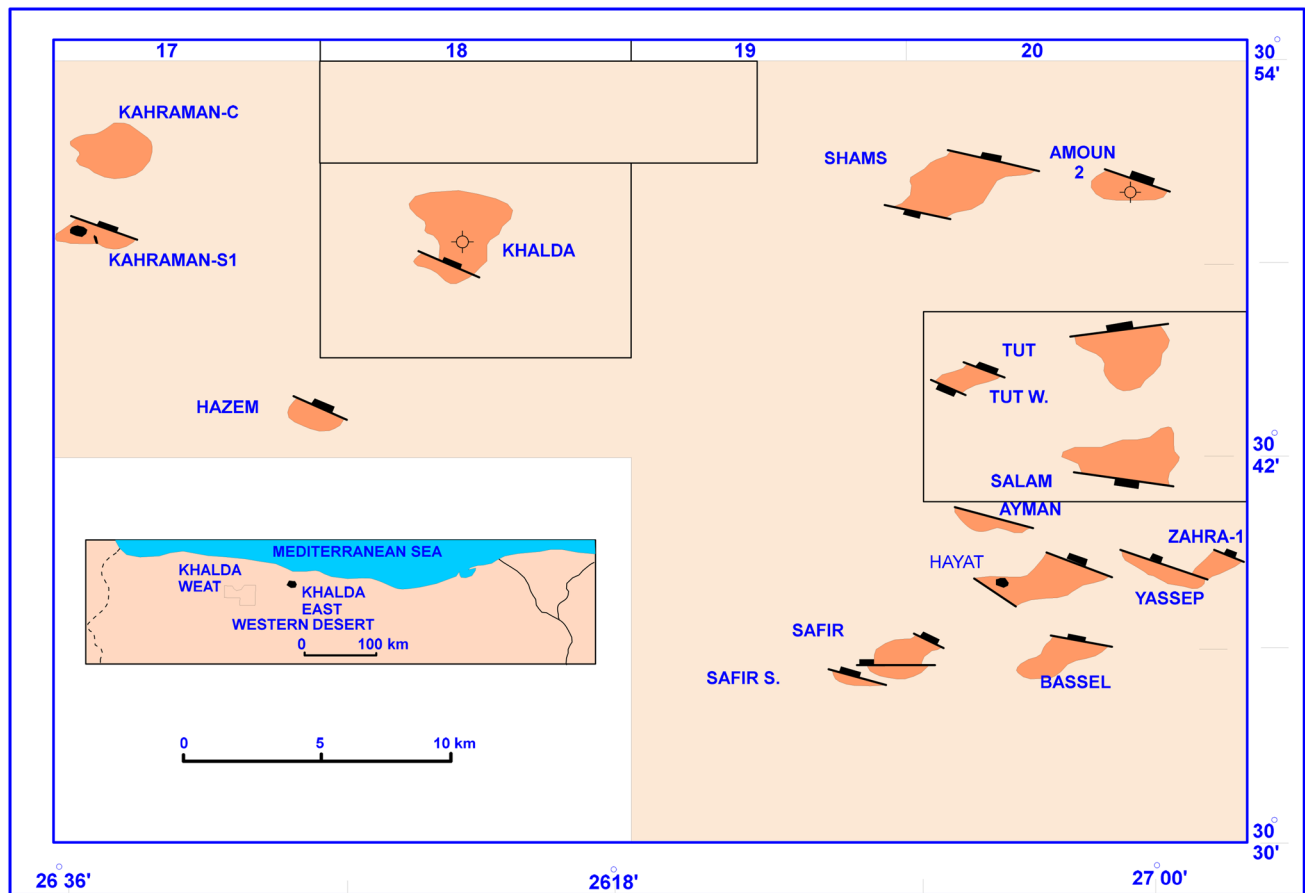


Fig. 4 Location map of the Khalda Field within the Khalda West Concession (Abed El Aziz 1994)

## Data and Methods

In this section, the available borehole logging data and the seismic lines will be listed and the applied methodology and techniques will be also discussed in some details.

### Petrophysical data

The formation evaluation and reservoir characterization is based on the petrophysical analysis of this formation (Shehata et al. 2021; Nabawy et al. 2022; Haque et al. 2022; Fallah-Bagtash et al. 2022). Consequently, for the present study, a complete set of borehole logs were released for five wells in Khalda Field (Kh\_45, Kh\_56, Kh\_58, Kh\_21x, and Kh-S-1 × wells, Fig. 7) crossing the Bahariya Formation including resistivity logs, neutron, density, PEF, and gamma-ray logs. The petrophysical analysis includes lithologic definition based on a set of X–Y cross-plots for the petrophysical parameters, and the litho-saturation vertical plot, and the contour maps of the petrophysical parameters in the different wells (Baouche and Nabawy 2021; Abdeen

et al. 2021). In this regard, the available well log data of the studied wells have been evaluated using the IP3.6 (Interactive Petrophysics); it is a proficient software applied to process and present the petrophysical well logging data as a function of depth and as a set of X–Y plots. The borehole and the environmental conditions were considered during the processing these petrophysical data using the Schlumberger charts (Schlumberger 1995; Nabawy and Shehata 2015; Radwan et al. 2021, 2022a, b).

### Lithology determination

Different methods were applied simultaneously to determine the lithology including the density-neutron, and the  $M$ – $N$  lithology identification cross-plots which were recommended by many authors (Radwan and Nabawy 2022). Estimating the  $M$  and  $N$  values is based on the apparent matrix density ( $\Delta m_a$ ) and the apparent transit time of rock matrix ( $\Delta t_{ma}$ ) as follows.

$$M = (\Delta T_f - \Delta T_{\log}) / (\rho_{\log} - \rho_f) \times 0.01 \quad (1)$$

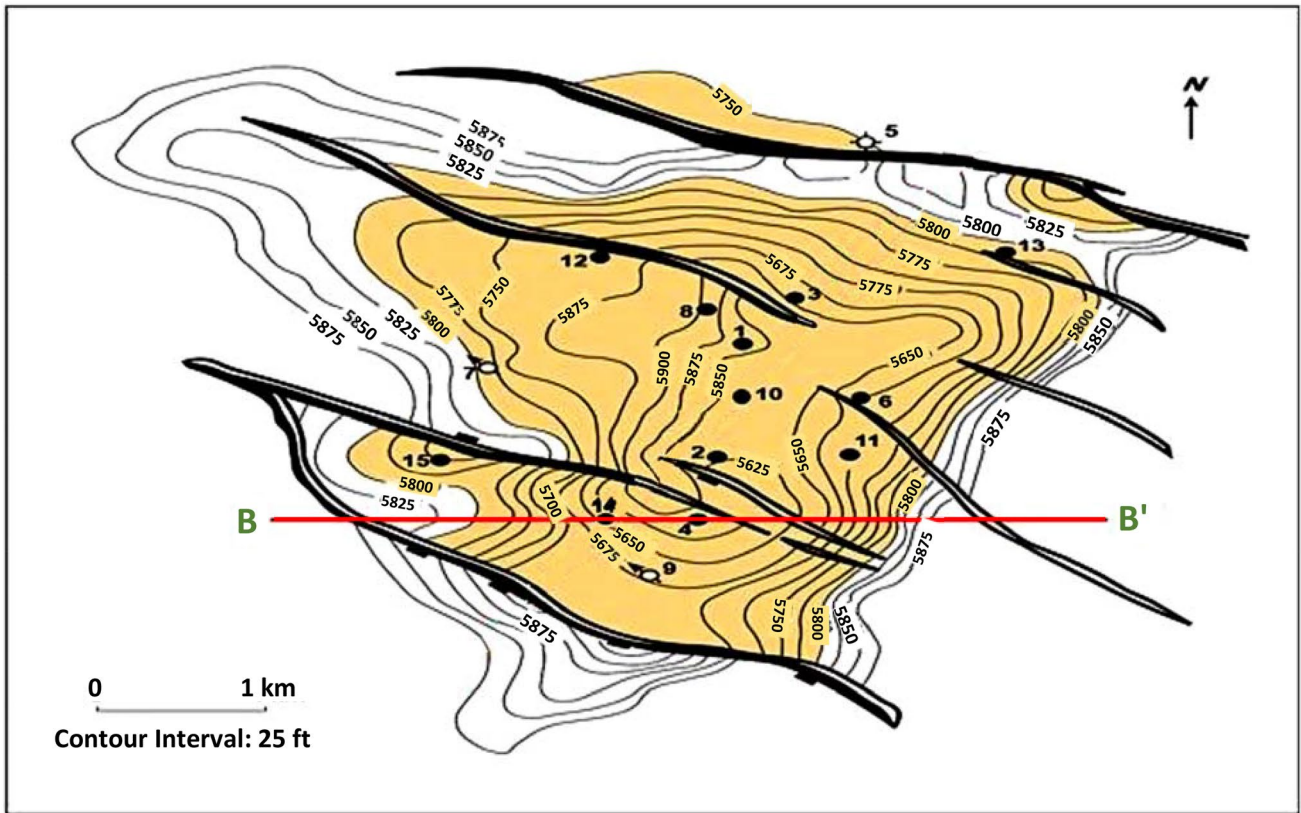


Fig. 5 Structural map on top of the Lower Bahariya Formation, Khalda Field (EGPC, 1992)

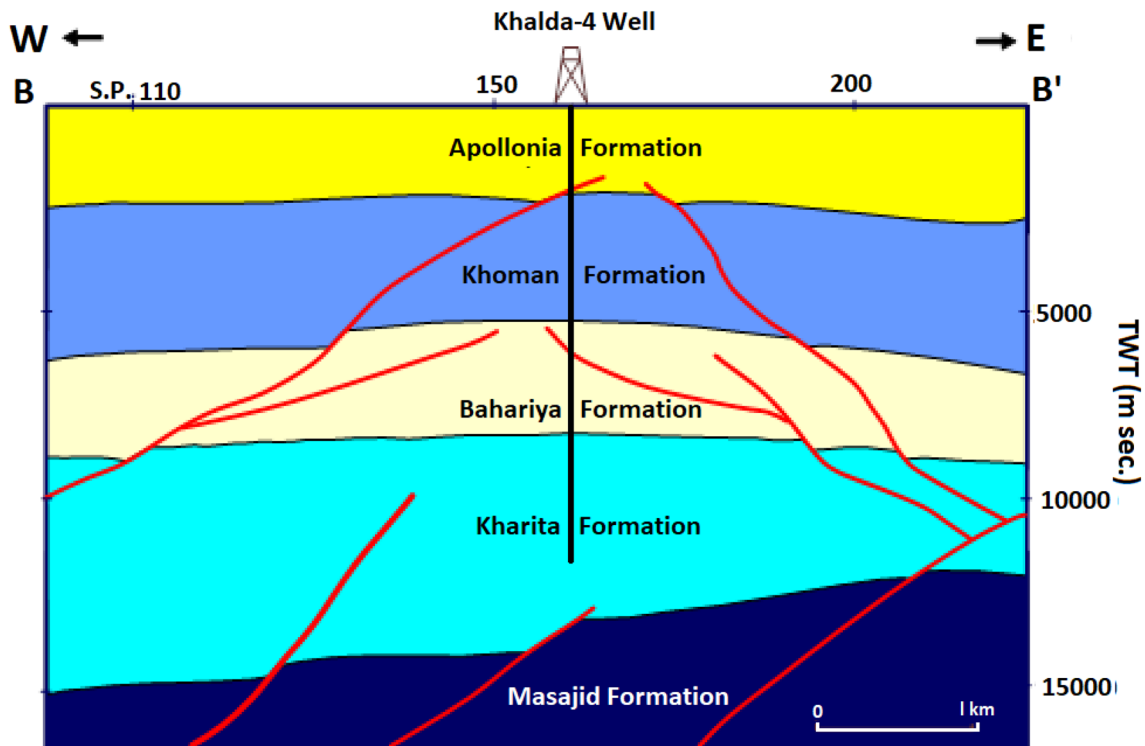
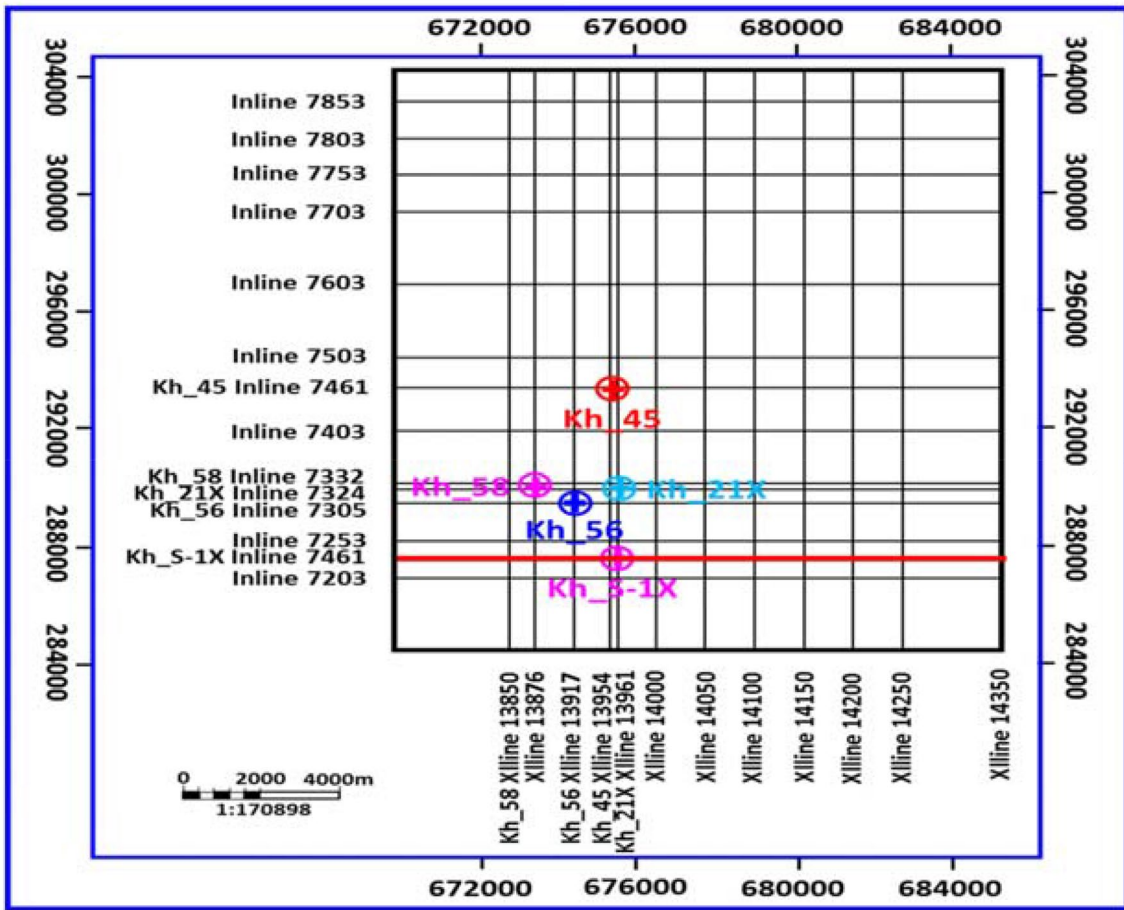


Fig. 6 E–W geoseismic cross section, crossing Khalda-4 well. Location is shown in Fig. 4



**Fig. 7** Seismic in-lines (E–W direction) and cross-lines (N–S direction) are shown on the Khalda Field location map. Locations of interpreted seismic sections are represented by colored lines

$$N = (\varnothing_{Nf} - \varnothing_{NL\log}) / (\rho_{Log} - \rho_f) \tag{2}$$

where  $\Delta T_f$  is the transit time of the saturating fluid,  $\Delta T_{Log}$  is the transit time log reading,  $\rho_{Log}$  and  $\rho_f$  are the density log reading and the fluid density, respectively,  $\varnothing_{Nf}$  is the neutron porosity of the saturating fluid, and  $\varnothing_{NL\log}$  is the porosity log reading.

**Shale volume determination (Vsh)**

Increasing the shale volume (Vsh) causes a reduction in the reservoir quality and the formation resistivity factor (David et al. 2015). The shale volume of the Bahariya Formation has been calculated using different techniques following Asquith and Gibson (1982) and Larionov (1969), and the most actual values were recorded as follows.

$$vsh = 0.083 \times (2^{3.7 \times (GRLog - GRmin)} / (GRmax - GRmin) - 1) \tag{3}$$

**Porosity estimation**

For the present study, the effective ( $\varnothing_e$ ) and total porosity ( $\varnothing_T$ ) values were calculated using the density-neutron values (Schlumberger 1995) as follows.

$$\varnothing_e = \varnothing_T (1 - V_{sh}) \tag{4}$$

$$\varnothing_T = (\varnothing_{NL\log} + \varnothing_{DL\log}) / 2 \tag{5}$$

where  $\varnothing_{NL\log}$  and  $\varnothing_{DL\log}$  are the neutron and density porosities.

**Water saturation (Sw)**

Due to the complexity of the reservoir lithologies and properties, different equations have been widely applied

to determine the water saturation ( $S_w$ ). Among these, the Simandoux's and the Indonesian equations are the most appropriate for the argillaceous clastic sequences ( $V_{sh} > 10\%$ ) like the Bahariya Formation (Simandoux 1963; Asquith and Krygowski 2004).

$$S_w = (a.R_w)/(2.\phi^m). \{ \text{SQRT}[(V_{sh}/R_{sh})^2 + ((4 * \phi^m)/(a.R_w.R_T))] - (V_{sh}/R_{sh}) \} \quad (6)$$

## Seismic data

For this study, a check-shot survey and a total of 27 seismic profiles (Fig. 7) covering the Khalda Oil Field and its dominant structure are available for the seismic data processing interpretation. The available data have a seismic bandwidth (10–70 Hz) and a reverse polarity. Also, the borehole logs helped in the well tie process to interpret the geologic and structural elements of Khalda Field. The seismic data were processed using the Halliburton Land-mark and Petrel software to perform the synthetic generation. The seismic data were grouped into stacks of the same orientation which means that the lines of the same stack have an orientation in the same dip direction of the major geologic features. The seismic interpretation workflow starting with collecting the seismic data and checking its quality and then the well tying, the fault and horizon interpretation, and the time to depth conversion process was applied to enable mapping the structural setting of the Khalda structure (Fig. 8).

In more details, the mapped structures and horizons were chosen considering their strength and continuity. Tying has been performed between wells and horizons that intersected them in the seismic profiles. Considering the fact that the present boreholes have been drilled vertically; so it is only require to get a correct check-shot point. The two-way travel time was converted into their equivalent depth points to present it correctly on the seismic section. After interpreting all the seismic profiles, the obtained information was then presented on a base map to construct a subsurface map for the

picked horizon. The most obvious type of data to get from the seismic profiles is the two-way travel time (TWT) of the picked surface that represents the mapped geologic horizon. It is the same technique for presenting the formation tops on a 2D map using the borehole log data. Additional useful information is detecting the up and down-thrown intersection points of a fault surface with the mapped horizon. Eventually, the TWT data are converted into depth values and contoured to present a structure contour map. All maps have been presented on a grid of Xinc 50 m x Yinc 50 m and contoured in a convergent interpolation.

## Results and interpretation

In this section, the obtained seismic results and interpretation will be discussed. This includes creating the synthetic seismogram to convert the time to depth domain, the seismic interpretation for detecting the dominant fault blocks and mapping the different seismic horizons of the tops of different interesting zones. Also, petrophysical results and interpretation of the borehole data will be discussed using a set of X–Y and litho-saturation plots.

### Synthetic seismogram

It is used to correlate between depths of the formation tops, as indicated from the well log data, and the picked horizons in the 2D seismic profiles. It is estimated from the borehole data and correlated with a particular seismic zone. The constructed seismogram is the principal link between the seismic and the borehole data, and it is the main tool that enables geological picking. This will be supported with a vertical sounding profile (VSP) as an alternative for the synthetic seismogram. In case of using combined density and acoustic logs for the studied borehole, the reflection coefficient is convolved with the wavelet to form the synthetic seismic trace.

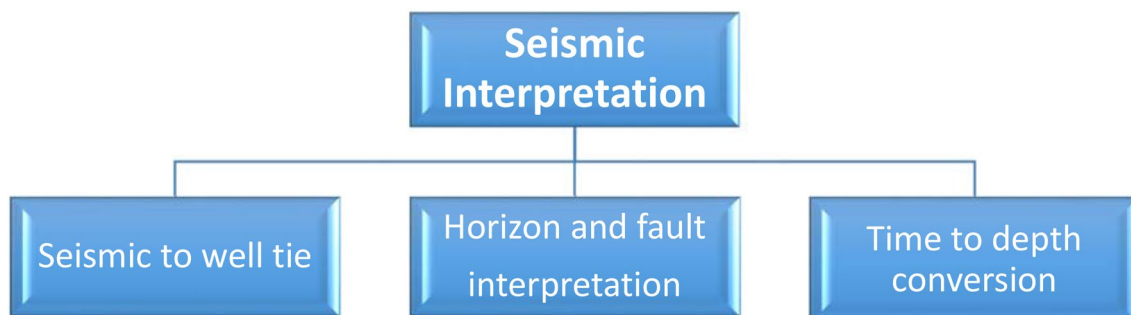


**Fig. 8** A sketch showing the seismic interpretation workflow starting with the seismic to well tie, horizon and fault interpretation, and time to depth conversion



In the present study, a set of synthetic seismograms were constructed for all wells that penetrated or crossed the seismic horizons. In general, tying between the seismic data and these synthetic seismograms were performed at a satisfactory level (Fig. 9). For example, the synthetic seismogram of KHALD-56 well indicates a successful general tying with the seismic data at the studied time zone in particular.

## Seismic interpretation

Interpreting the seismic data of the subsurface sequences delineates both the geological and the structural features which are presented on the seismic profiles as extended horizons. On contrary, faults are presented as discontinuities in these horizons (Abd-El Gawad et al. 2015; Abdeen et al. 2021).

In Khalda structure, the Cretaceous section was interpreted on the seismic sections covering the Khalda Oil Field. It is indicated that the Upper Cretaceous Abu Roash and the Lower Cretaceous Alam-El Bueib formations have been affected by normal faulting. Though the implication of folding is minimized, it is traceable in the field. The E–W and NW–SE gravity faults are detectable in the seismic in-lines along the E–W direction (Figs. 10 and 11). These in-line profiles show a gravity faulting with a folded structure along its downthrown side. This is due to the fact that there is an elongated folded structure affected by faulting along this level (Fig. 10). The fold extends along the NE–SW direction while faulting extends in the NW–SE direction which is in accordance with the structural regime of the north WD of Egypt during the Late Cretaceous (Moustafa 2008).

For the present study, the normal faults are primarily represented by steep fault surfaces dipping from 60°

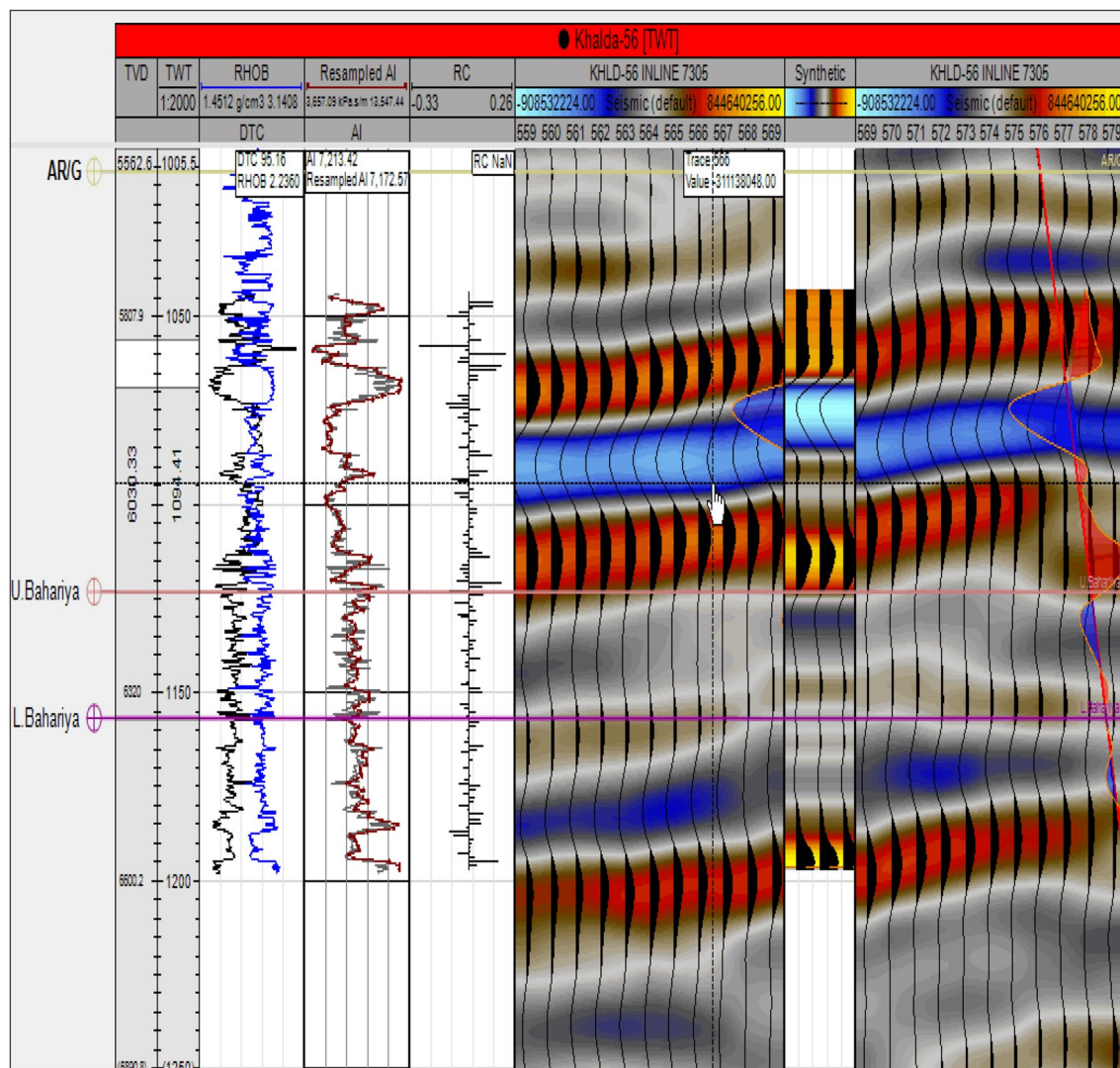
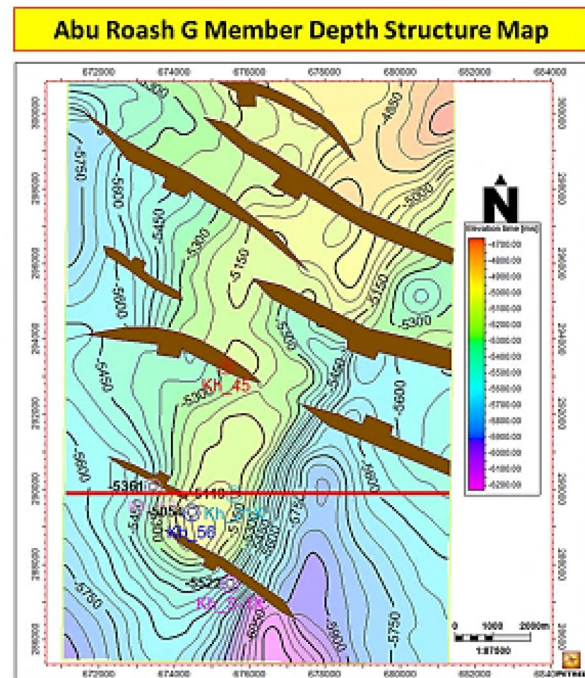
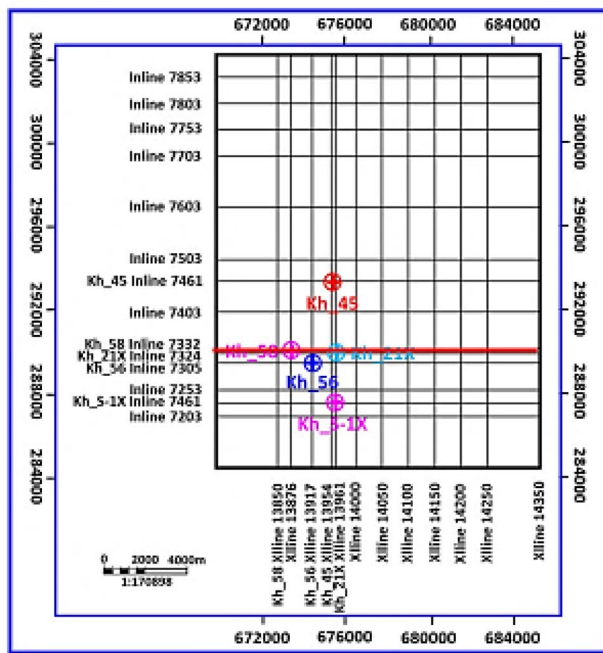
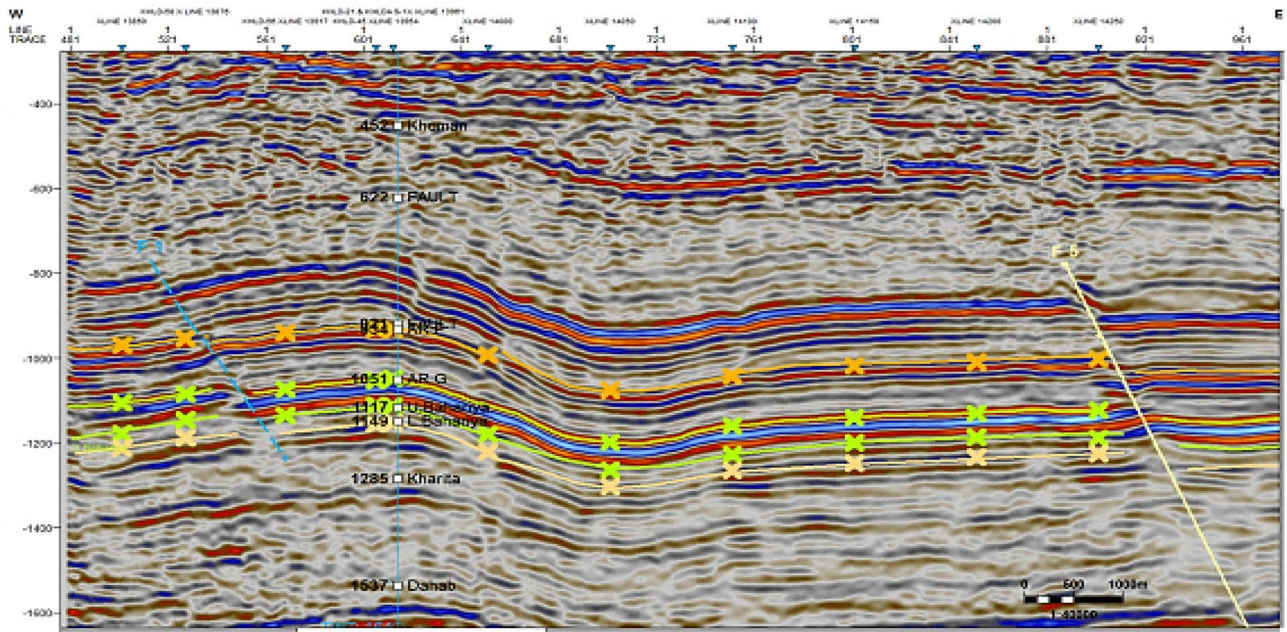


Fig. 9 A synthetic seismogram created for the Khalda-56 well



**Fig. 10** The interpreted TWT seismic section that E–W and pass through the Kh\_58 well. It shows a normal faulting with a somewhat folded structure along its downthrown side. The fault trends NW–SE direction with its dip direction toward NE

to 70°. Clustering the gravity faults in groups can create some low and high-standing fault blocks as shown in the rifted crest of the Khalda structure (Fig. 11). These faults are commonly recognized crossing the Miocene and the Pre-Miocene sequences. The dominant structural style trends to the northwest-southeast direction.

**Fault blocks**

For the present study, the fault blocks which are bounded from the different sides by fault surfaces which are widely presented in the central parts of Khalda structure. The triggering mechanisms of these fault blocks are referred to the

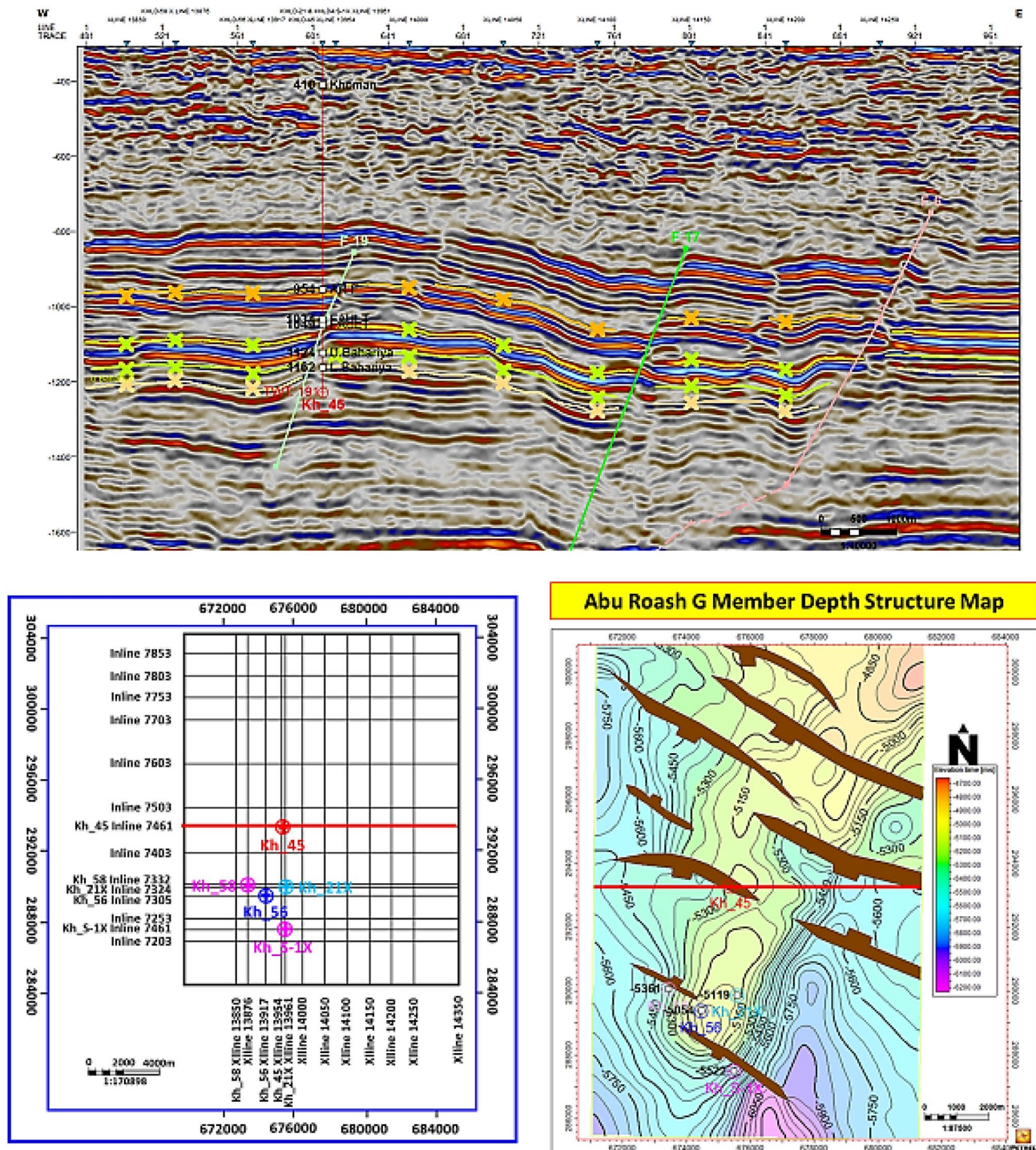


Fig. 11 The interpreted TWT (msec.) seismic section that extends along the E–W direction passing through the Kh<sub>45</sub> well. The interpreted depth structure map on top of the Abu Roash G member is shown to the right down corner of the figure

Miocene event. The majority of these blocks are tilted toward the depositional basin of the Bahariya Formation, sometimes are rotated backwards. The top of these blocks are overlain by sandstone alternated with shale sediments. In general, Khalda structure is dissected by some northwest-southeast

gravity faults that bound the northward tilted blocks of some half-grabens (Figs. 10 and 11). Also, the N–S direction profiles indicate simplicity of the dominant structures represented by simple normal faults and grabens of slight throws and horizontality of the bedding planes (Fig. 12).

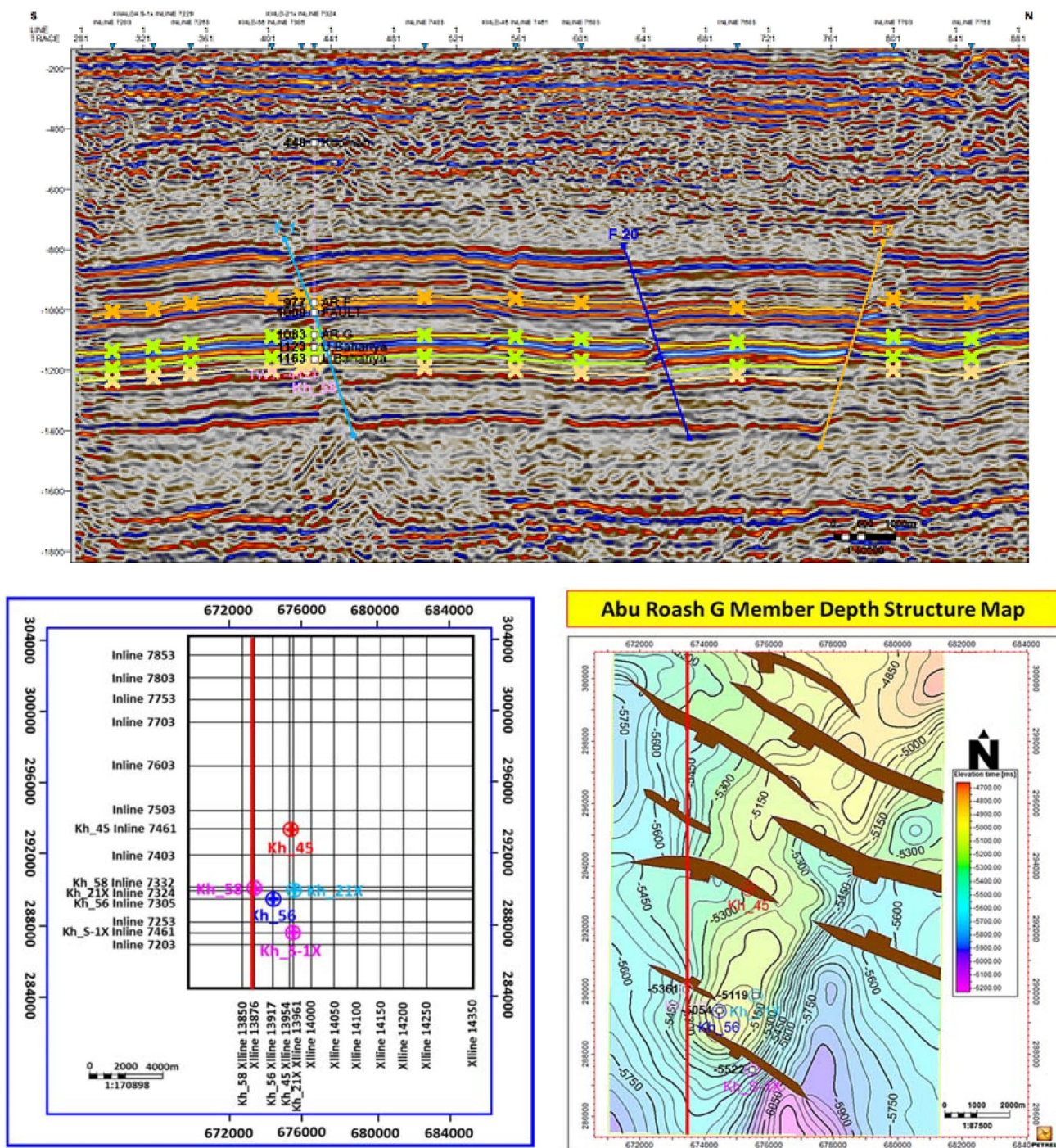


Fig. 12 The Interpreted TWT (msec.) seismic section that extends along the S–N direction, and passing through the KH\_58 well. Interpreted and un-interpreted TWT (msec.) Seismic Section (XLINE 13,850), extend along the S–N direction, and passing through KH\_58 well

**The subsurface structural maps**

Four horizons were mapped for top surfaces of the Lower and Upper Bahariya members, and the Abu Roash F and G members (Figs. 13, 14, 15 and 16). The mapped structure contour surfaces indicate the presence of some large-scale

NE–SW major gravity faults trending with a few NW–SE gravity faults. Additional major E–W branching gravity fault lies to S of the Khalda structure. These aforementioned step-gravity faults dissect the main hydrocarbons-bearing structure into some tilted blocks which are deeper to the north and shallower to the south. A three-way

### Abu Roash F Member Depth Map

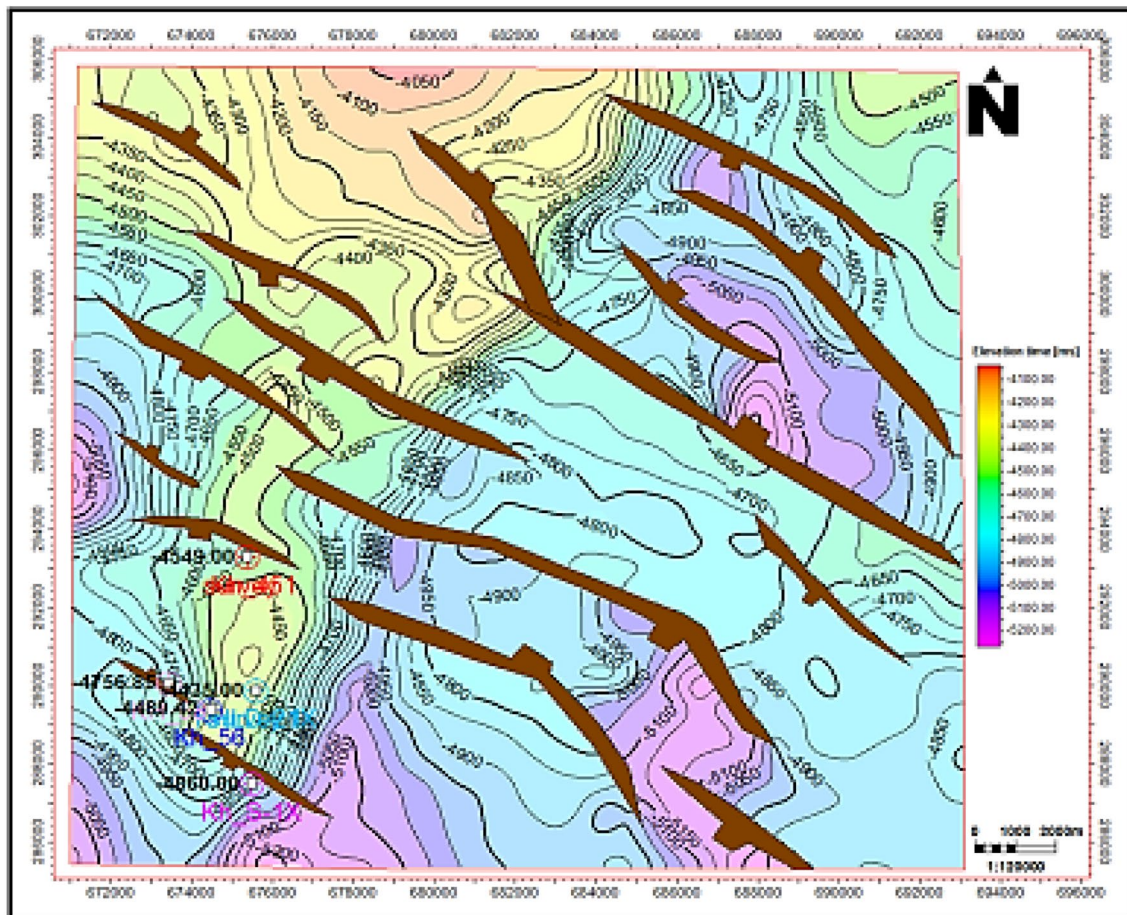


**Fig. 13** The depth structural contour map on the top of Abu Roash F member (C.I= 100 ft)

structural closure has been appeared in some parts due to the intersection of these structural blocks forming some faulted anticlines. These structural closures are caused due to the vertical basement movements.

**Abu Roash F (ARF) member** The depth structure contour map for the upper surface of the Abu Roash F Member, as derived from the 2D seismic data, indicates the presence of two major fault trends (NE–SW and NW–SE) with more dominance for the NW–SE trend (Fig. 13). These faults are NW–SE gravity faults with its down throw to the east forming step zone faults and a half-graben structure. The structural setting of the ARF Member is structurally high in most parts of the Khalda Field, while highest location extends from the central to the western parts and recording a depth interval 3500–5000 ft subsea. On the other hand, a low structure is presented along the NE direction and extends down to depth 5800 ft at the deepest point of the basin.

**Abu Roash G (ARG) member** The depth structure contour map for the upper surface of the Abu Roash G Member, as derived from 2D seismic data, shows the dominance of two main fault trends (NE–SW and NW–SE) with more dominance for the NW–SE trend (Fig. 14). The structural configuration of the upper surface of the ARG Member is structurally high area in most parts, recording the smallest depth values ranging from – 5700 ft in the central parts to – 4500ft to the SW. The low stand areas are situated in the eastern parts of the study area with the deepest site reaching down to – 6800 ft depth. The faults are NW–SE gravity faults with the main throw located to the east forming step zone faults and a half-graben structure.

The major faults trend NW–SE directions in the study area with its down throw oriented to the east direction in some major faults and to the west direction in the other faults. These major faults were created with the seismicity initiation in the Khalda Field. The depocenter location of the depositional basin of this Cretaceous sequence is mainly

### Abu Roash G Member Depth Map

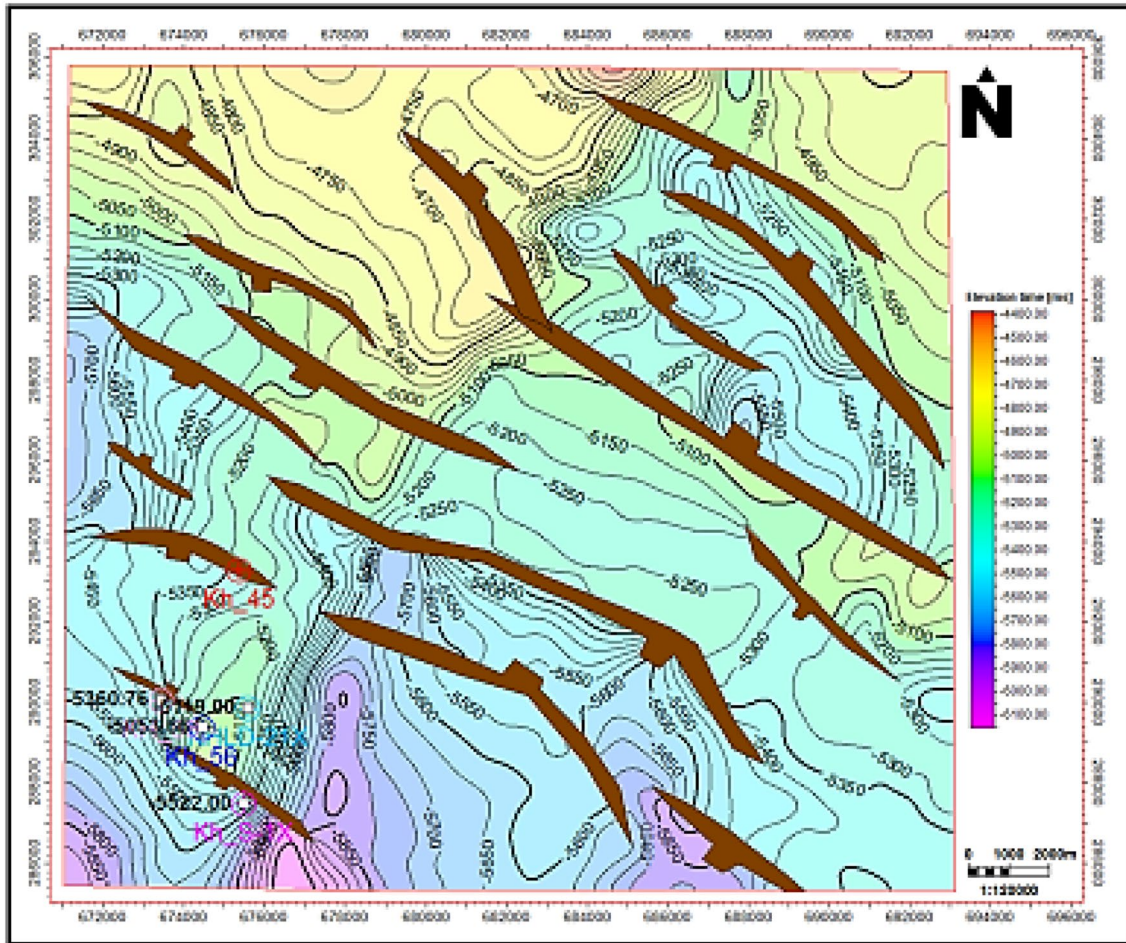


**Fig. 14** The depth structural contour map on top of the Abu Roash G member (C.I= 100 ft)

situated in the southeastern parts of the Khalda Field. The major trend of the Abu Roash formation is NW–SE trend that is of the implementation of the clismic system. The top of the ARG represents the main reservoir in some wells of the Khalda Field.

**Upper Bahariya member** The depth structure map of the top surface of the Upper Bahariya Member, as created from the 2D seismic data, shows that it is structurally high area (Fig. 15). Its lowest depth values are recorded between depths – 5500ft in the western, and – 7350 ft in the central part, while the highest depth is recorded in the southern parts with depth values down to – 8800ft. Most faults are trending NW–SE with some cross elements which directed along the NE–SW trend but with decrease in the faults intensity.

**Lower Bahariya member** The depth structure contour map on upper surface of the Lower Bahariya Member indicates that the structural high stand areas are represented by the lowest depth values between – 5500 ft in the western side, and – 7350 ft in the central part, while structurally low areas are located in the southern part of the area recording the highest depth values at – 8800ft (Fig. 16). The predominant faulting trend is NW–SE with some cross elements which directed the fault patterns in the NE–SW but with less faulting intensity. The Lower Bahariya Formation is the main producing reservoir in this area.

Therefore, the depth intervals and their increase or decrease directions of the depth structure maps for the different horizons that were abovementioned are tabulated in Table 1. It indicates that the minimum contour values are primarily observed to the southwestern parts of the study

## Upper Bahariya Depth Map

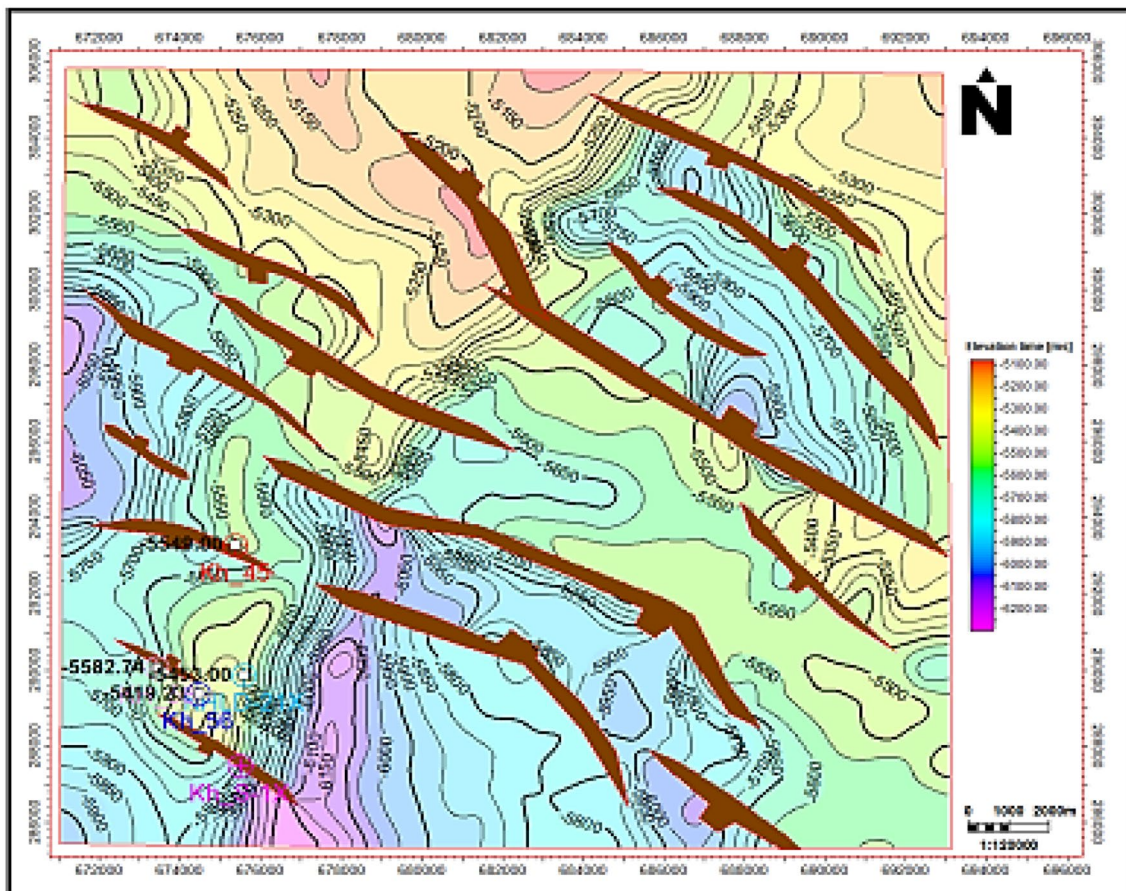


**Fig. 15** Depth structure contour map on the top Upper Bahariya Formation in the study Area (C.I= 100 ft)

area, while the maximum contour values are observed to the north of the study area.

### Petrophysical results and interpretation

#### Results

Due to the prospectivity of the Albian-Cenomanian Bahariya Formation as indicated from the seismic study and the well log data, its petrophysical properties and reservoir characteristics were studied in detail. The total gross thickness of the Bahariya Formation including its upper and lower members is estimated as 383–415 ft in the studied wells (Table 2). Due to the structural setting and situation of the Kh\_45 and Kh\_S-1 × wells in as low stand in a graben between two normal faults as indicated for the seismic profiles (Fig. 12), it is fully saturated with water and indicates not oil prospectivity which primarily migrated in accumulated in the high stand

sites in the center of the structure at the crest of the anticline (at kh\_56 and kh\_58 wells, Fig. 10). The petrophysical analysis of the estimated net-pay thickness, including the shale volume, the net to gross, the effective values, and the water saturation, indicates that the shale volume is less 32.2%, the water saturation is less than 59.0% (for Kh\_56, Kh\_58 and Kh\_21X wells), while the effective porosity is more than 16% up to 25% (Table 2). To estimate the net-pay thickness and based on the well testing data, 10% porosity, 35% shale volume and 70% water saturation were applied as cutoff values. Based on these cutoffs, a total net-pay thickness equals is estimated as 18 to 38 feet in the center of the structure (Table 2). These prospective reservoir properties and the oil saturation resulted in a good  $\Phi \cdot H$  values (the weighted reservoir pore volume) vary between 1.79 and 3.68. The Bulk volume of water BVW ( $\Phi \cdot S_w$ ) varies between 0.08 and 0.25. The obtained petrophysical and reservoir properties are tabulated in Table 2.

### Lower Bahariya Depth Map

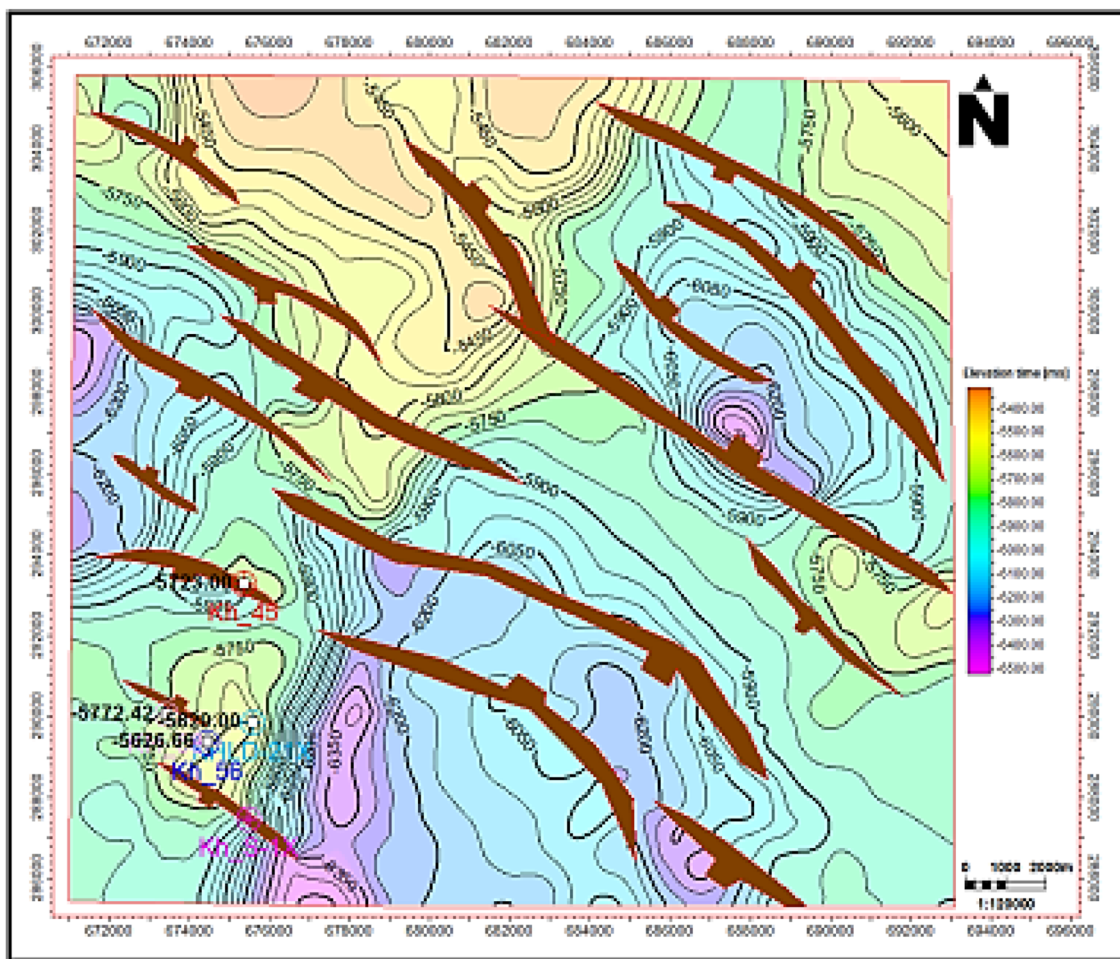


Fig. 16 Depth structure contour map on the top Lower Bahariya Formation in the study area (C.I= 100 ft)

**Table 1** The main parameters of the depth structure maps on top of the Abu Roash F and G members, as well as the Upper and Lower Bahariya members the study area

Boundary Name	Depth interval (ft.)	Increase direction	Decrease direction	Comments
Abu Roash F Member	3500–5800	East	West	The youngest reflector, affected by faults
Abu Roash G Member	4500–6900	East	West	The second older boundary in the study area
Upper Bahariya Member	5600–9000	East-southeast	West–northwest	Normal faulting started from pre- Miocene and extended until the
Lower Bahariya Member	5400–9300	East- southeast and central parts	Northwest	Normal faulting during the late-Miocene

#### Interpretation

The variation of the petrophysical properties and reservoir parameters of the Bahariya Formation is primarily

attributed to its structural complicated setting in the Khalda Field which is controlled by a series of normal faults forming a horst (Fig. 6), graben (Fig. 12), anticline (Fig. 10), and a step-fault zone (Fig. 11). Consequently, to



**Table 2** The net-pay reservoir parameters derived from the borehole log data of the Bahariya Formation, Khalda Field

Well	Units	Top (ft)	Bottom (ft)	Gross (ft)	Net (ft)	N/G 0.00	$\varnothing_{\text{eff}}$ 0.00	Sw 0.00	Vsh 0.00	Phi*H 0.00	Phi*Sw 0.00
Kh-45	U Bah	6323	6503	180	–	–	0.25	1.00	0.14	–	0.25
	L Bah	6503	6800	236	–	–	0.22	1.00	0.06	–	0.22
Kh-56	U Bah	6192	6405	213	15	0.070	0.19	0.54	0.171	2.85	0.10
	L Bah	6405	6575	170	23	0.135	0.16	0.53	0.185	3.68	0.08
Kh-58	U Bah	6353	6527	174	10	0.056	0.21	0.58	0.06	2.10	0.12
	L Bah	6527	6700	173	12	0.68	0.19	0.53	0.11	2.28	0.10
Kh_21X	U Bah	6189	6391	202	7	0.035	0.25	0.59	0.322	1.79	0.15
	L Bah	6391	7189	798	11	0.014	0.21	0.55	0.311	2.26	0.11
Kh_S-1X	U Bah	6618	6796	178	–	–	0.19	0.99	0.236	–	0.19
	L Bah	6796	7292	496	–	–	0.18	0.99	0.155	–	0.18

where  $N/G$  is the net to gross ratio,  $\varnothing_{\text{eff}}$  is the effective porosity,  $Sw$  is the water saturation ratios,  $Vsh$  is the shale volume, and  $H$  is the net-pay thickness

check the lithology composition and to match the promising reservoir zones a set of X–Y plots and litho-saturation plots are presented and discussed in the following section.

**X–Y plots** To determine the lithology of the studied sequence, a set of X–Y plots including the density-neutron, and the M–N plots were presented in accompany with the gamma-ray (GR) values (Fig. 17a, b). The density-neutron plot for the lower and upper members of the Bahariya reservoir sequence in the kH\_45 well indicates that all the measured points have porosity higher than the cutoff value (10%) up to 30% and that the readings are shifted toward higher carbonate content with GR fluctuating between 30 and 120 API with most values locates between 60 and 90 API. The API values are higher for the Upper Bahariya Member (Fig. 17a), than that for the Lower Bahariya Member (Fig. 17b).

These relatively high GR readings may be attributed to the relatively high content of siltstone in the rock phase and the U content in the water content. Also, the GR values are due to the presence of many shale streaks especially in the Upper Bahariya Member which has been deposited in estuarine to shallow marine environment as referred by many authors (Shehata et al. 2018, 2020, 2021; Nabawy et al. 2022). Nabawy et al. (2022), in their studies on the mineral composition of the Bahariya sequence in Shushan Basin, referred that the Bahariya sequence is relatively rich in K-feldspars (up to 19.2%), glauconite (up to 11.2%), and pyrite content (up to 8.1%) as revealed from the XRD data. This relatively high content of the K-feldspars and accessory minerals causes a decrease in the resistivity values and increase in the GR readings even in the oil-bearing zones (Nabawy et al. 2022). So, it is recommended in the future exploration plan to apply the spectral gamma logging to enable estimating the corrected GR values.

Also, plotting the M–N values on X–Y plot (Fig. 18a, b) for the Upper and Lower Bahariya Members in the Kh\_56

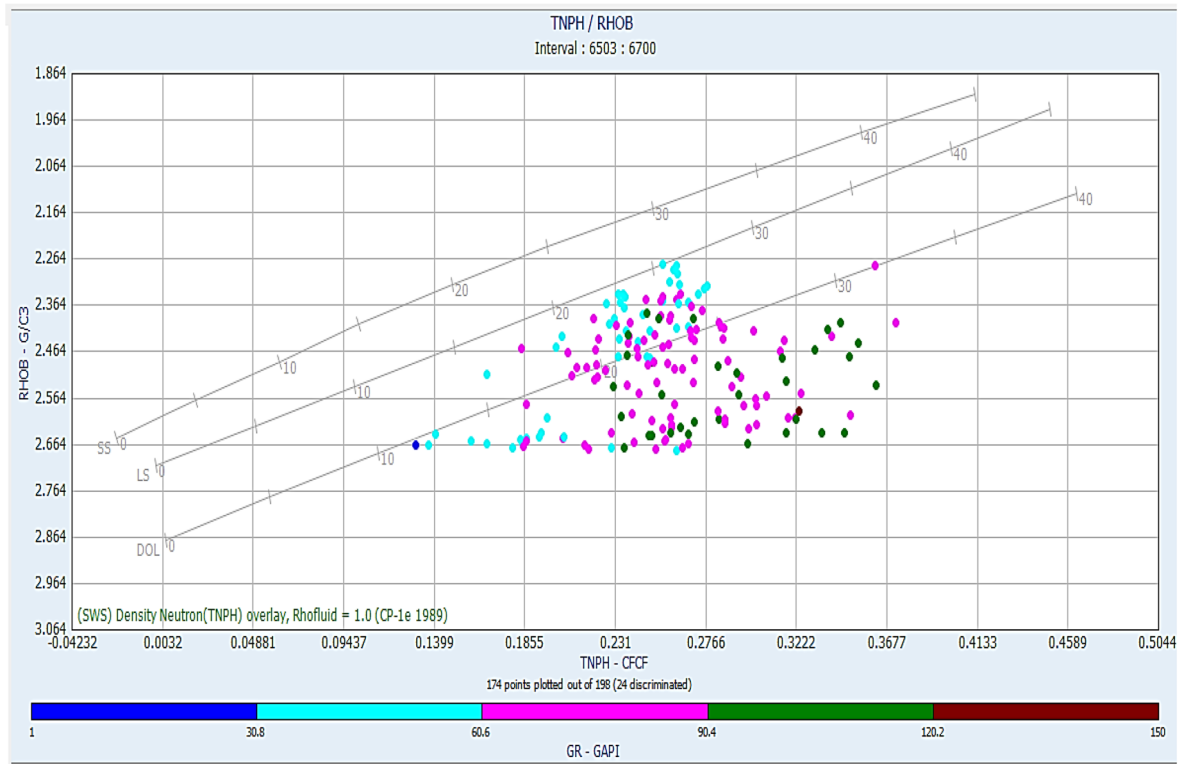
well indicates that the measured points are characterized by relatively moderate to high GR readings (almost 30–90 API). It is also indicated that the measured points are shifted toward the higher carbonate content with relatively high  $Ca^{+2}$  and  $Mg^{+2}$  content with more shift for the upper member (Fig. 18b) than the lower member (Fig. 18a). Decreasing the  $M$  and  $N$  values may be also attributed to the relatively high acoustic and neutron porosity readings for the measured points. The silt and the carbonate content may be thought to play a main role in this behavior.

### Litho-saturation plots

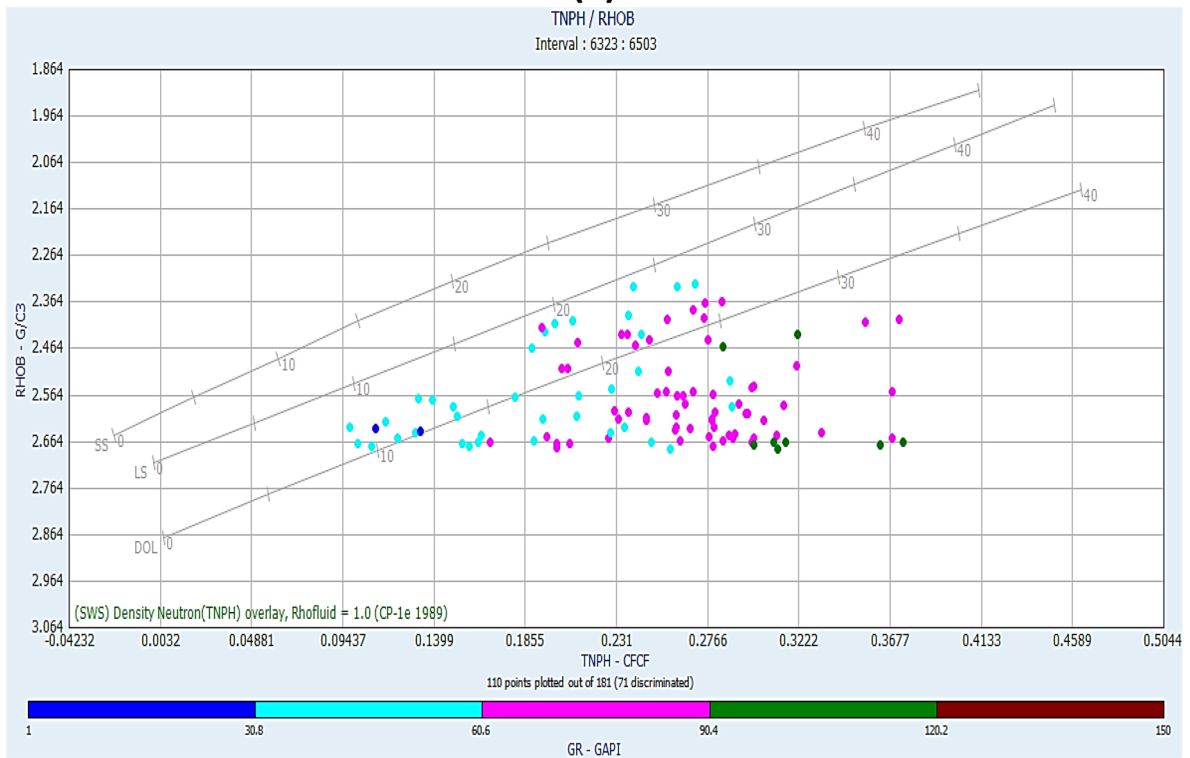
The litho-saturation plot of the Kh\_45 and the Kh\_56 wells indicates different petrophysical properties of both the upper and lower members of the Bahariya Formation with relatively high GR values up to 120 API (Fig. 19a, b). Plotting the petrophysical values of the Kh\_45 well indicates relatively higher shale content in the upper member than the lower one where a few thin sand interbeds are recorded in the upper member (Fig. 19a).

In spite of increasing the porosity with increasing the sand content (tracks 6 and 10), the bulk volume of water (BVW) increases which is attributed to the full saturation of this sequence by water, i.e., it is beneath the OWC in the study area. As aforementioned, this may be attributed its low stand position, so it is recommended to avoid exploration to the NE direction where the Kh\_45 is situated in a graben structure.

On moving to the SW and central parts of the study area where the anticline crest at the Kh\_56 well (Fig. 19b) and the Kh\_58 well, the sand content increases in both the upper and the lower members which caused increasing the potentiality of the Bahariya Formation to trap hydrocarbons. So, many movable hydrocarbons-bearing zones are assigned through the different levels of the sequence. Increasing the

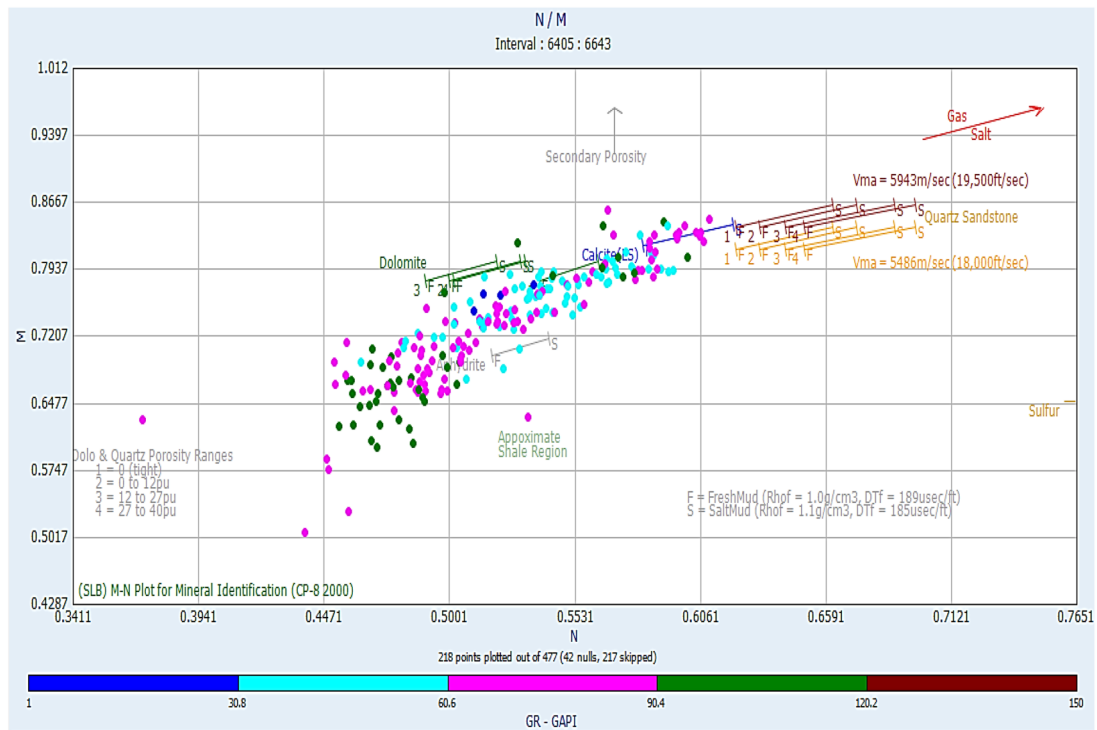


(a)

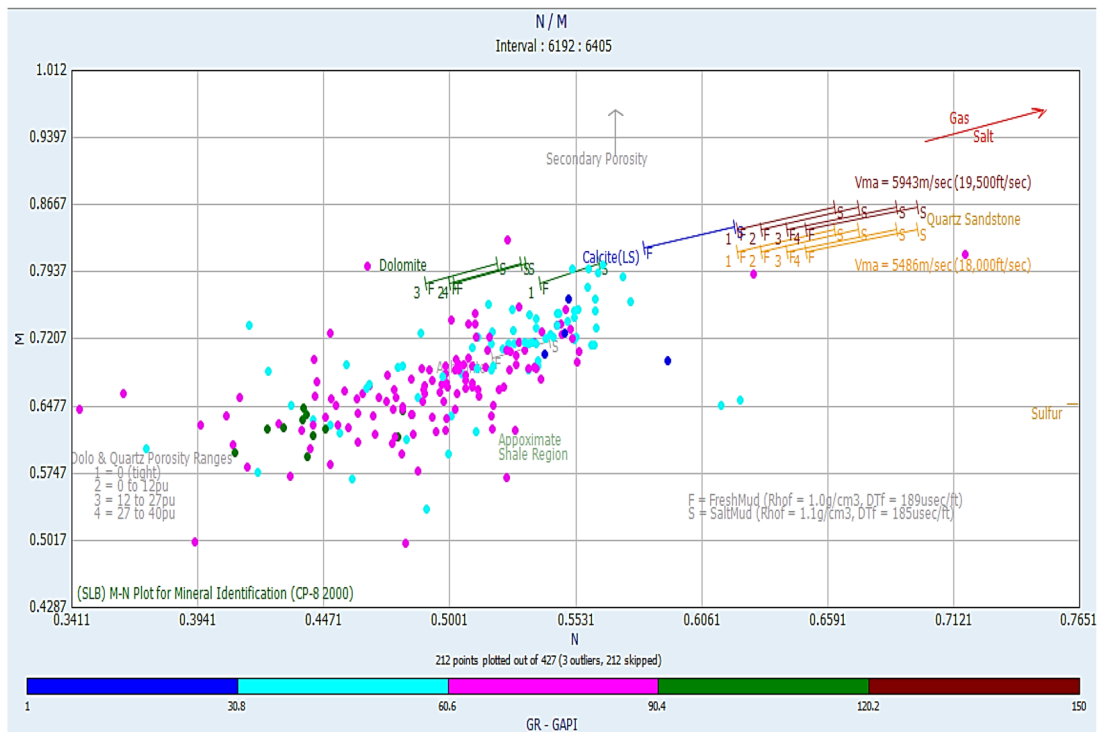


(b)

Fig. 17 Neutron-Density (TNPH-RHOB) cross-plots for **a** the Lower Bahariya Member, and **b** the Upper Bahariya Member in Kh\_45 well



(a)



(b)

Fig. 18 M–N cross-plots for **a** the Lower Bahariya Member, and **b** the Upper Bahariya Member in Kh\_56 well

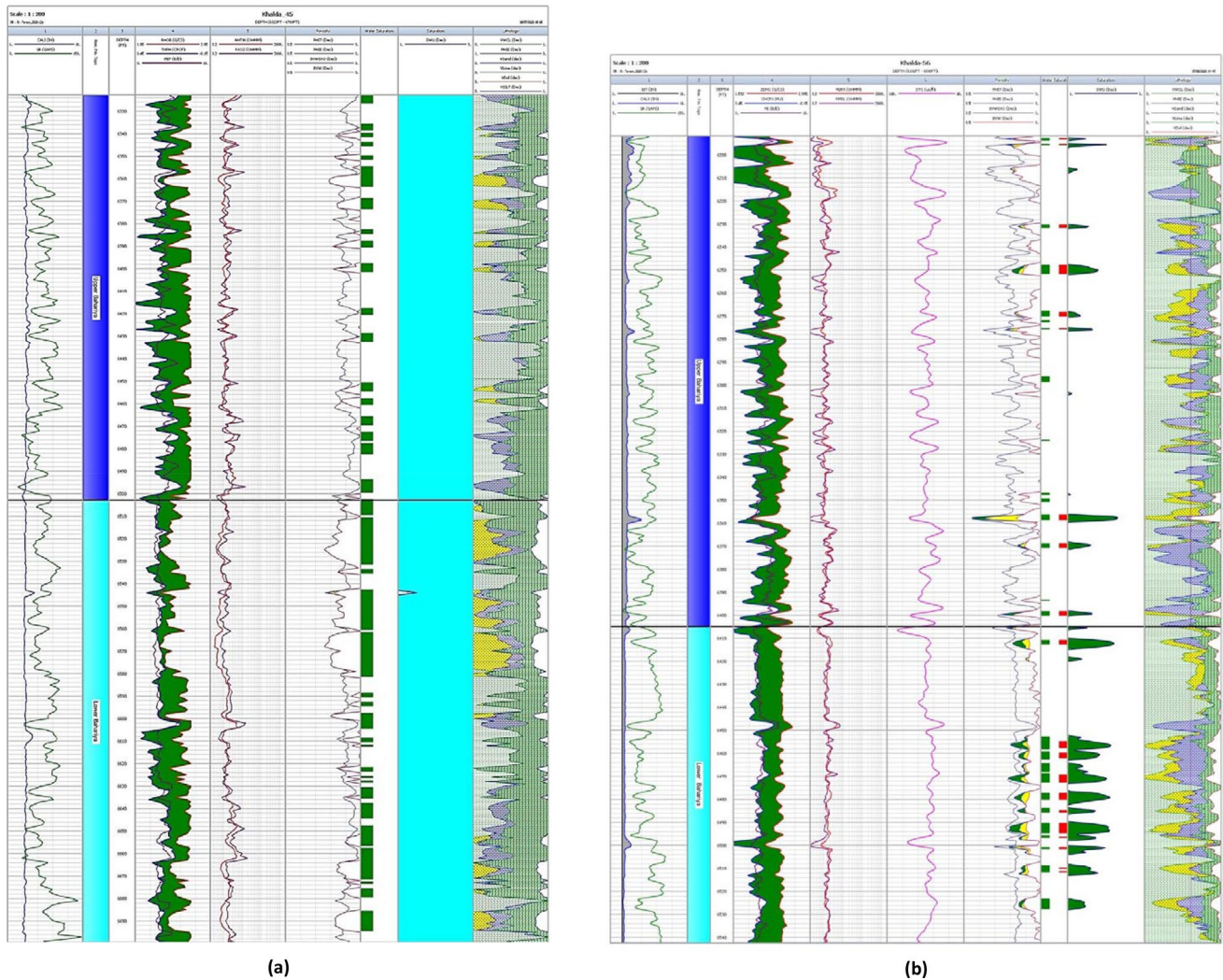


**Fig. 19** Litho-saturation cross-plots of the Bahariya Formation, showing the lithology, total and effective, shale volume, porosity, water saturation and net pay zones for **a** Kh\_45 well, and Kh\_56 well

potentiality of the Bahariya Formation in the Kh\_56 well increases the net-pay thickness to 38 ft. The BVW data of this well are relatively low causing low water cut production. The relatively low deep resistivity values in both wells though being the Kh\_45 well a water-producing while the Kh\_56 are a hydrocarbon producing well indicates that the relatively high glauconite and pyrite content is more effective in reducing the resistivity values than that of the saturating interstitial hydrocarbons which tend to increase the resistivity values.

## Regional applications

The Albian-Cenomanian deposits are a promising reservoir sequence in the Western Desert, Egypt, and in NE Africa. So, they are studied by many authors during the last decades. The present integrated petrophysical and seismic study

is considered an additional study conducted on the highly prolific Albian-Cenomanian Bahariya and Abu Roash reservoirs which are widely distributed in the different promising basins of the Western Desert and produce most of the oil production of the Western Desert (Nabawy and ElHariri 2008; Shalaby et al. 2008; Bosworth et al. 2015; Teama and Nabawy 2016; Gentzis et al. 2018; Nabawy et al. 2022). As a result, the present study on this sequence is extendable to other extensions and subsurface equivalents in Egypt and NE Africa. The low resistivity values of the studied Upper Bahariya Member even in the oil-bearing zones are due of the presence of glauconite, pyrite, and conductive clay minerals which may be considered an ideal case for low resistivity reservoirs and can be applied to other similar case studies in the vicinity. As a result of this low resistivity phenomenon and the relatively high heterogeneity of the Bahariya Formation, more advanced processing techniques such

as the artificial neural network (ANN) should be applied in further petrophysical studies to avoid the overestimated water saturation in these low resistivity hydrocarbon-bearing sequences. This advanced technique should be run in parallel to another advanced technique to reveal the real mineral composition this type of argillaceous, glauconitic and pyritic reservoirs.

## Conclusions

- Processing and interpreting the seismic data enabled figuring out the structural setting of the Cretaceous sequence in Shushan Basin based on a synthetic seismogram which indicating high reflectors strength and reflection coefficient.
- Interpreting the seismic profiles delineated the implication of the normal faulting on the Albian-Cenomanian Bahariya reservoirs creating a number of horsts and grabens of slightly tilted blocks and limited throws.
- Seismic achievements are supported by the petrophysical properties of the Lower and the Upper Bahariya members that revealed the presence of some prospective zones in both members with a potential net-pay thickness (18–38.0 ft). The porosity ( $\phi_e$ ), shale volume ( $V_{sh}$ ) and the water saturation ( $S_w$ ) of the Bahariya sequence are promising ( $\phi_e \geq 16\%$ ,  $V_{sh} \leq 32.2\%$ , and  $S_w \leq 59.0\%$ ).
- Finally, delineating the prospectivity of the Albian-Cenomanian Bahariya clastics in Shushan Basin using the proposed workflow is applicable to their subsurface extensions in the other basins in the Western Desert, NE Africa, and the NW parts of the Arabian Peninsula.

**Acknowledgements** We wish to express our most sincere gratitude and appreciation to the Egyptian General Petroleum Corporation (EGPC) and Khalda Petroleum Company (KPC) for their kind cooperation and permission to use, process, and publish the released data of this paper. Also, the authors would like to thank the editor-in-Chief Prof Dr. Ali Ghalambor and the anonymous reviewers for their valuable and constructive comments and recommendations that highly improved the manuscript in its present version.

**Funding** Open access funding is provided by The Science, Technology & Innovation Funding Authority (STDF) in cooperation with The Egyptian Knowledge Bank (EKB).

## Declarations

**Conflict of Interest** The authors confirm that they do not have a financial or personal relationship with any party who are interested in this study or could be positively or negatively influenced by the article's content.

**Open Access** This article is licensed under a Creative Commons Attribution 4.0 International License, which permits use, sharing, adaptation, distribution and reproduction in any medium or format, as long

as you give appropriate credit to the original author(s) and the source, provide a link to the Creative Commons licence, and indicate if changes were made. The images or other third party material in this article are included in the article's Creative Commons licence, unless indicated otherwise in a credit line to the material. If material is not included in the article's Creative Commons licence and your intended use is not permitted by statutory regulation or exceeds the permitted use, you will need to obtain permission directly from the copyright holder. To view a copy of this licence, visit <http://creativecommons.org/licenses/by/4.0/>.

## References

- Abed El Aziz AL (1994) Jurassic source rock maturity and thermal history modeling of Khalda west area, North Western Desert, Egypt. EGPC 12th Petrol. Explor. Prod. Conf., Cairo 1:217–233
- Abdelmaksoud A, Radwan AA, (2022) Integrating 3D seismic interpretation, well log analysis and static modelling for characterizing the Late Miocene reservoir, Ngatoro area, New Zealand. Geomechanics and Geophysics for Geo-Energy and Geo-Resources vol 8, Article number: 63.
- Abdeen MM, Ramadan FS, Nabawy BS, El Saadawy O (2021) Sub-surface structural setting and hydrocarbon potentiality of the komombo and nuqra basins, south Egypt: a seismic and petrophysical integrated study. Nat Resour Res 30(5):3575–3603
- Abd-El Gawad EA, Elsheikh A, Afify W, Salem T (2015) Petroleum system evaluation of jurassic and paleozoic sections in Faghur Basin, north Western Desert, Egypt. IJSEAS 1
- Abdelmaksoud A, Amin AT, El-Habaak GH, Ewida HF (2019) Facies and petrophysical modeling of the upper bahariya member in abu gharadig oil and gas field, North Western Desert Egypt. J Afr Earth Sci 149:503–516
- Abdou A (1998) Deep wells in Khalda West—a brief review In: proceedings 14th petroleum conference EGPC, Cairo, Exploration 2 517–533
- Abu Shady AN, Ahmed Moustafa El-Shishtawy AM, Abdel Hameed AT, Abdelkader T (2010) Reservoir Characterization of the Upper Cretaceous Bahariya Formation, Khalda Ridge, North Western Desert, Egypt. Conference In: proceedings 6th international symposium on geophysics, Tanta, Egypt
- Almoqaddam RO, Darwish M, EL-Barkooky AN, Clerk C (2018) Sedimentary facies analysis of the Upper Bahariya sandstone reservoir in East Bahariya C area, North Western Desert Egypt. Egypt J Pet 27(4):1103–1112
- Asquith G, Gibson C (1982) Basic well log analysis for geologists. The american association of petroleum geologists. AAPG Methods in Exploration Series, No. 16
- Asquith G, Krygowski D (2004) Basic well log analysis. AAPG Methods in Exploration Series 16 2004
- Baouche R, Nabawy BS (2021) Permeability prediction in argillaceous sandstone reservoirs using fuzzy logic analysis: a case study of Triassic sequences, Southern Hassi R'Mel Gas Field, Algeria. J African Earth Sci 173:104049
- Bosworth W, Drummond M, Abrams M, Thompson M, (2015) Jurassic rift initiation source rock in the Western Desert, Egypt-relevance to exploration in other continental rift systems. Petroleum Systems in “Rift” Basins, 34th Annual GCSSEPM Foundation Perkins-Rosen Research Conference 13–16
- David C, Bertauld D, Dautriat J, Sarout J, Menéndez B, Nabawy B (2015) Detection of moving capillary front in porous rocks using X-ray and ultrasonic methods. Front Phys 3:53. <https://doi.org/10.3389/fphy.2015.00053>

- EGPC (Egyptian General Petroleum Corporation) (1992) Western desert oil and gas fields In: EGPC 11th petroleum exploration and production conference, Egypt
- Emujakporue G, Nwankwo C, Nwosu L (2012) Integration of well logs and seismic data for prospects evaluation of an X field, Onshore Niger Delta Nigeria. *Int J Geosci* 3(4A):872–877. <https://doi.org/10.4236/ijg.2012.324088>
- Fallah-Bagtash R, Adabi MH, Nabawy BS, Omidpour A, Sadeghi A (2022) Integrated petrophysical and microfacies analyses for a reservoir quality assessment of the Asmari Dolostone sequence in the Khesht Field, SW Iran. *J Asian Earth Sci* 223:104989
- Genzits T, Carvajal-Ortiz H, Deaf A, Tahoun SS (2018) Multi-proxy approach to screen the hydrocarbon potential of the Jurassic succession in the Matruh basin, north Western Desert Egypt. *Int J Coal Geol* 190:29–41
- Hassan A, Abdel Meguid A., Waheed S, Salah M, Abdel Karim E (2015) Multistage horizontal well hydraulic fracturing stimulation using coiled tubing to produce marginal reserves from brownfield: case histories and lessons learned. SPE Middle East Unconventional Resources Conference and Exhibition, 26–28 January, Muscat, Oman <https://doi.org/10.2118/172933-MS>
- Haque AKM, Qadri SMT, Bhuiyan A, Navid M, Nabawy B, Hakimi MH, Abd-El-Aal AK (2022) Integrated wireline log and seismic attribute analysis for the reservoir evaluation: a case study of the Mount Messenger Formation in Kaimiro Field, Taranaki Basin, New Zealand. *J Nat Gas Sci Eng* 99:104452
- Kassab MA, Abbas AE, Attiya AS (2019) Hydrocarbon potential of Upper Bahariya member in Um Baraka oil field, North Western Desert Egypt. *NRIAG J Astron Geophys* 8(1):204–219
- Larionov VV (1969) Borehole radiometry: Moscow. Nedra, U.S.S.R
- Maity D, Aminzadeh F (2015) Novel fracture zone identifier attribute using geophysical and well log data for unconventional reservoirs. *Interpretation* 3(3):T155. <https://doi.org/10.1190/INT-2015-0003.1>
- Maity D, Aminzadeh F (2012) Reservoir characterization of an unconventional reservoir by integrating microseismic, seismic, and well log data. Paper presented at the SPE Western Regional Meeting, Bakersfield, California, USA. SPE-154339-MS. <https://doi.org/10.2118/154339-MS>
- Mohamed AK, Ghazala HH, Mohamed L (2016) Integration between well logging and seismic reflection techniques for structural analysis and reservoir characterizations, Abu El Gharadig basin Egypt. *NRIAG J Astron Geophys* 5(2):362–379. <https://doi.org/10.1016/j.nrjag.2016.07.003>
- Moustafa AR (2008) Mesozoic-Cenozoic Basin evolution in the northern western desert of Egypt In: Salem M, El-Arnauti A, and Saleh A (ed) 3rd symposium on the sedimentary basins of libya (The Geology of East Libya) 3: 29–46
- Nabawy BS, ElHariri TYM (2008) Electric fabric of cretaceous clastic rocks in Abu Gharadig basin, Western Desert Egypt. *J Afr Earth Sci* 52(1–2):55–61
- Nabawy BS, Shehata AM (2015) Integrated petrophysical and geological characterization for the Sidi Salem-Wakar sandstones, offshore Nile Delta Egypt. *J Afr Earth Sci* 110:160–175
- Nabawy BS, Lashin AA, Barakat MKh (2022) Implementation of lithofacies and microfacies types on reservoir quality and heterogeneity of the Late Cretaceous Upper Bahariya Member in the shrouk field, Shoushan Basin, north Western Desert Egypt. *J Asian Earth Sci* 224:105014
- Radwan AA, Nabawy BS (2022) Hydrocarbon prospectivity of the Miocene-Pliocene clastic reservoirs, Northern Taranaki basin New Zealand: integration of petrographic and geophysical studies. *J Pet Explor Product Technol*. <https://doi.org/10.1007/s13202-021-01451-4>
- Radwan AA, Nabawy BS, Abdelmaksoud A, Lashin A (2021) Integrated sedimentological and petrophysical characterization for clastic reservoirs: a case study from New Zealand. *J Nat Gas Sci Eng* 88:103797
- Radwan AA, Abdelwahhab MA, Nabawy BS, Mahfouz KH, Ahmed MS (2022a) Facies analysis-constrained geophysical 3D-static reservoir modeling of Cenomanian units in the Aghar Oilfield (Western Desert, Egypt): insights into paleoenvironment and petroleum geology of fluviomarine systems. *Mar Pet Geol* 136:105436
- Radwan AA, Nabawy BS, Shihata M, Leila M (2022b) Seismic interpretation, reservoir characterization, gas origin and entrapment of the Miocene-Pliocene Mangaa C sandstone, Karewa Gas Field, North Taranaki Basin New Zealand. *Mar Pet Geol* 135:105420. <https://doi.org/10.1016/j.marpetgeo.2021.105420>
- Rossi C, Marfil R, Ramseyer K, Permanyer A (2001) Facies-related diagenesis and multiphase siderite cementation and dissolution in the reservoir sandstones of the Khatatba Formation Egypt's Western Desert. *J Sediment Res* 71(3):459–472
- Schlumberger (1995) Well evaluation conference, Algeria, 56–87
- Sehim AA, Shettia IA, El Nahass MR (1992) Proposed structural model Khaldia West Concession, Western Desert—Egypt. In: Proceedings 11th Exploration & Production Conference, EGPC, Cairo, Exploration 2:79–97
- Shalaby MR, Abdullah WH, Abu Shady AN (2008) Burial history, basin modeling and petroleum source potential in the Western Desert. *Egypt Bull Geol Soc Malays* 54:103–113. <https://doi.org/10.7186/bgsm54200817>
- Shehata AA, El Fawal FM, Ito M, Abdel Aal MH, Sarhan MA (2018) Sequence stratigraphic evolution of the syn-rift early cretaceous sediments, west Beni Suef basin, the Western Desert of Egypt with remarks on its hydrocarbon accumulations. *Arab J Geosci* 11:313–331
- Shehata AA, El Fawal FM, Ito M, Aboulmagd MA, Brooks HL (2020) Senonian platform-to-slope evolution in the tectonically-influenced Syrian Arc sedimentary belt: Beni Suef Basin Egypt. *J Afr Earth Sci* 170:103934. <https://doi.org/10.1016/j.jafrearsci.2020.103934>
- Shehata AA, Osman OA, Nabawy BS (2021) Neural network application to petrophysical and lithofacies analysis based on multi-scale data: an integrated study using conventional well log, core and borehole image data. *J Nat Gas Sci Eng* 93:104015. <https://doi.org/10.1016/j.jngse.2021.104015>
- Simandoux P (1963) Dielectric measurements in porous media and application to shaly formation, revue del'institut francais du petrole, Supplementary Issue 193–215
- Teama MA, Nabawy BS (2016) Petrophysical evaluation of the hydrocarbon potential of the Lower Cretaceous Kharita clastics, North Qarun oil field, Western Desert Egypt. *J Afr Earth Sc* 121:62–71
- Wang X, Zhang B, Zhao T, Hang J, Wu H, Yong Z (2017) Facies analysis by integrating 3D seismic attributes and well logs for prospect identification and evaluation—a case study from Northwest China. *Interpretation* 5(2):1M-T277. <https://doi.org/10.1190/INT-2016-0149.1>

**Publisher's Note** Springer Nature remains neutral with regard to jurisdictional claims in published maps and institutional affiliations.